UNIVERSITY OF CALIFORNIA

Los Angeles

Verification modeling study for the influential factors of secondary clarifier

A thesis submitted in partial satisfaction

of the requirements for the degree Master of Science

in Civil Engineering

by

Haiwen Gao

2016

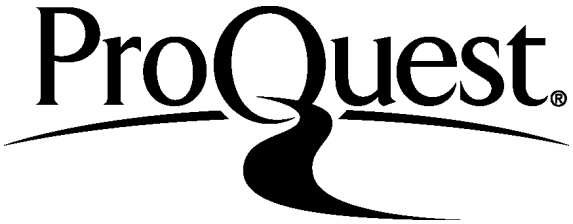

ABSTRACT OF THE THESIS

Verification modeling study for the influential factors of secondary clarifier

by

HAIWEN GAO

Master of Science in Civil Engineering

University of California, Los Angeles, 2016

Professor Michael K. Stenstrom, Chair

A numerical Quasi 3-D model of secondary clarifier is applied to verify the data obtained through the literature and analyze the influential factors for secondary clarifiers. The data from the papers provide the input parameters for the model. During this study, several influential factors (density waterfall; surface overflow rate; solids loading rate; solids-settling characteristics; mixed liquor suspended solid; clarifier geometry) are tested. The results show that there are some differences and consistence between the simulation data obtained from the Quasi 3-D model and the simulation outcomes revealed in the papers.

Key Words: Quasi 3-D model; secondary clarifier; influential factors

The thesis of Haiwen Gao is approved.

Jennifer A. Jay

William W-G. Yeh

Michael K. Stenstrom, Committee Chair

University of California, Los Angeles

2016

Table of Contents

List of Figures

Appendix Figures

List of Tables

Nomenclature

K_1= empirical coefficient for rapid settling floc resulting from fit of batch settling data $(g/L)^{-1}$;

K_2= a settling exponent for the poorly settling particles $(g/L)^{-1}$;

C_{min}= the concentration of non-settling floc (g/L);

V_o= Stokes velocity (settling velocity of single particle in clear water) (m/h);

MLSS= concentration of the mixed liquor suspended solids (g/L);

V_c= compression settling velocity (m/h);

Kc= compression settling parameter $(g/L)^{-1}$;

Q_{in}= influent flow rate (m^3/h);

Q_r= returned flow rate (m^3/h);

SLR= solids loading rate ($kg/m^2 \times h$);

RAS Ratio= return activated sludge ratio;

SOR= surface overflow rate (m/h);

1. Introduction

Effluent suspended solids (ESS) from biological processes, such as the activated sludge process, are affected by the performance of secondary clarifiers or secondary settling tanks (SSTs). Since escaping solids contain contaminants, like BOD, COD, heavy metals, nitrogen and phosphorus, the removal efficiency of SSTs is fundamental to the overall performance of a wastewater treatment plant (Parker et al., 1996). As noted by Kleine and Reddy (2005), there are two different functions of SSTs: clarification and thickening. Clarification is used to separate the suspended solids (SS) from the effluent; thickening is the process to concentrate the sludge in order to recycle or dispose of it in a small volume. The failure in clarification or the thickening processes, which usually results from not understanding of the two-phase nature of the flow, will result in violations of the effluent permits and biomass loss (Ben and Stenstrom, 2014). Moreover, it may be more complicated with the existence of hydrodynamic and physical effects, such as density currents and flocculation (Kleine and Reddy, 2005). Therefore, SSTs designed by a simple rule such as surface overflow rate (SOR) and hydraulic retention time (HRT) are problematic, and many other influential factors, such as inlet and outlet structures, tank geometry, wind movement, rainfall, concentration of mixed liquor suspended solids or density gradients, and temperature should be taken into account (Wang et al., 2011).

This thesis reviews current SST literature with particular regard to mathematical models. Recent advances in computer technology have made the use of computational fluid dynamics (CFD) a practical alternative for SST analysis and design. A brief review of CFD models is presented, showing their evolution from early models in the 1980s to advanced three dimensional models in current use. An analysis of circular SSTs is provided using a public domain computer

code developed by McCorquodale and his coworkers (McCorquodale et al., 2005). The code is used to analyze several SST designs presented by others and compares the functions and efficiencies of different design aspects, such as baffles and other geometries.

2. Literature Review

SST research was first performed more than 100 years ago and many significant advances were made. Recent work with CFD models refines and improves some of this earlier work. The review provided in this thesis is restricted to the use of modeling techniques to improve SST performance. For a more detailed review of all aspects of SSTs, the reader is referred to (McCorquodale et al., 2004; De Clercq (2003); Ben and Stenstrom, 2014).

CFD models have generally analyzed the effects of geometry such as flocculating wells, energy dissipate inlets (EDI) and peripheral baffles. For inlet baffle study, Fan et al. (2007) discussed the influence of the baffle height and baffle location on the distribution of solid concentrations and found that the inclusion of the baffle was helpful for the accumulation of suspended solids. Wang et al. (2011) and Liu et al. (2013) also modeled the baffle height and location and obtained an optimal value for the specific secondary clarifier. Ramalingam et al. (2009) studied different baffles in the same tank and found a preferred baffle installation in the SSTs in WWTPs in New York City. Although changes of baffle height, location and configuration have a great influence on the ESS, the optimal baffle parameters may only be suitable for tanks with similar structures (Fan et al., 2007).

Geometry such as the size of flocculation zone, the depth and total size of the SSTs has a direct impact on the performances of clarifiers. Vitasovic et al. (1997) observed that by reducing the size of the flocculating well from 46% to 28% of the tank diameter, the ESS decreased from 87mg/L to 15mg/L. Parker et al. (1996) stated that flocculating well size between 32% and 35% of the side wall radius produced the lowest ESS. In addition, a deeper SST can mitigate the blanket encroachment problem and stabilize its performance in a high SOR (Parker et al., 2001).

In order to understand the relationship between SOR, SLR and ESS, Vitasovic et al. (1997) analyzed the ESS for different parallel simulations. The results showed that both SOR and SLR impacted the ESS. In addition, Wahlberg et al. (1998) investigated the data from Vitasovic et al. (1997), and observed that SLR, rather than SOR, was the most significant loading parameter that affects secondary clarifier performances. What's more, Parker et al. (1996) discovered that the performance of WWTPs was very stable over a very broad range in overflow rates. In his later research (Parker et al., 2001), he explained that the existence of a correlation between SOR and ESS indicated either a problem on design or operation existed. So far, no solid conclusion has been made on the impact of SOR on ESS. More investigations, therefore, need to be performed.

Moreover, the effect of density currents, which is caused by a fluid flowing into an ambient fluid of a different density, on the performances of SSTs should not be neglected (Amir and Schroeder, 2000). However, the causes of density currents are controversial (Amir and Schroeder, 2000). Moursi et al. (1995) suggested that the density currents may occur from thermal effects, concentration effects, and the release of gas bubbles. However, Amir and Schroeder (2000) mentioned that the formations of density currents in the tank were independent of the amount of influent SS. His experiment showed temperature appeared to be the dominant factor of density currents in secondary clarifiers. Zhou and McCorquodale (1992) concluded that a temperature difference, as small as 0.2^{o}C, could result in the formation of density currents. In addition, research by Amir and Schroeder (2000) indicated that the type of surface or bottom density currents depended on temperature difference between influent and tank contents. Due to the controversial conclusions made by different researches, more studies are required to better understand the essential causes of density currents in SSTs.

With the development of computer technology and mathematical models, computational fluid dynamics (CFD) software has become an efficient tool to predict and verify the performances of wastewater treatment reactors (Fan et al., 2007). In this study, the 2Dc (Quasi 3-D axisymmetric) unsteady state secondary settling tank model package from New Orleans University is used for simulation and the outputs are displayed using TECPLOT (Bellevue, WA 98015). The general information for the computer used for this study are shown below:

CPU--Intel Core i7, 5500U, @ 2.40GHz 2.40GHz.
RAM--16.0GB
OS—windows 10, 64-bit.

A total of 104 simulations were performed during this study, and it takes the computer 12 minutes to get the result of each simulation. The objectives of this study are to understand the effect of several influential factors, for instance SOR, SLR, tank geometry variation and density currents on the concentration of ESS and to analyze the modeling outputs by comparing the simulation results with the field data and the simulation outcomes in the papers.

3. Description of Conditions and the Tested Clarifier

A full-scale, center-feed, peripheral withdrawal circular tank (Figure 1) was tested using a number of conditions provided by Vitasovic et al. (1997) and Wahlberg et al. (1998). Firstly, the verification of the 2Dc model was performed with the results presented in Table 1 and plotted in Figure 2. The simulations show good agreement with the field data.

Next, different influential factors were evaluated and were summarized in Tables 2 through 6. The simulation time for all the conditions was 400 minutes, which was the same as the simulation time in Vitasovic et al. (1997). "NA" means the model fails to output the results for the specific condition. A red value means the result did not reach the equilibrium and ESS was still rising after 400 minutes of steady input.

The Tables 1 through 5 show the input parameters used in Vitasovic et al. (1997) research. In Table 1, the lower six rows show the pervious experimental results and the new 2Dc model results. In Tables 2 to 4, the lower six rows show the previous model results and the new 2Dc model results. In Table 5, the input parameters are shown in the first two rows, except the last two columns in the second row. The new 2Dc modeling results are shown in the last two columns. In Table 6, the data in the matrix 1 (simulations 41 through 56) and the first two groups of data in the matrix 2 (simulations 57 through 64) were obtained from Wahlberg et al. (1998). The last two groups of data in the matrix 2 (simulations 65 through 72) are the additional data added in this study, where the SOR ranges between the first two groups of the matrix 2. In the last two columns, the pervious experimental results and the 2Dc model results are shown.

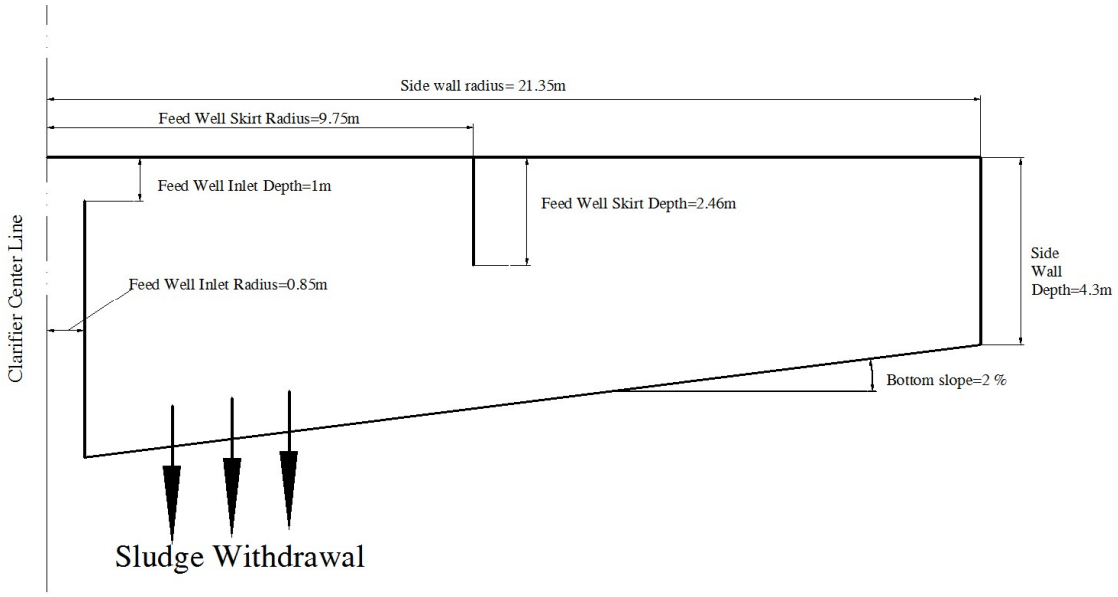

Figure 1. Geometry of the tested clarifier

In Table 1, the inputs of the five data points are shown from rows 2 through 13, which are from K_1 to SOR. The previous experimental results and 2Dc modeling results in this study are shown in the last six rows. These five data points are numbered as the first five simulations in this study. The velocity and solids distribution profiles for these five simulations are listed in Figures 3(a) to 7(a) in Appendix and streamline profiles are shown in Figures 3(b) to 7(b) in Section 4.1, respectively. The definitions of the input parameters are listed bellow:

K_1= empirical coefficient for rapid settling floc resulting from fit of batch settling data $(g/L)^{-1}$;

K_2= a settling exponent for the poorly settling particles $(g/L)^{-1}$;

C_{min}= the concentration of non-settling floc (g/L);

V_o= Stokes velocity (settling velocity of single particle in clear water) (m/h);

MLSS= concentration of the mixed liquor suspended solids (g/L);

V_c= compression settling velocity (m/h);

Kc= compression settling parameter $(g/L)^{-1}$;

Q_{in}= influent flow rate (m^3/h);

Q_r= returned flow rate (m^3/h);

SLR= solids loading rate ($kg/m^2 \times h$);

RAS Ratio= return activated sludge ratio;

SOR= surface overflow rate (m/h);

Table 1-Selected clarifier simulation conditions used for modeling verification (Vitasovic et al., 1997)

Simulations	1	2	3	4	5
$K_1(g/L)^{-1}$	0.62	0.65	0.67	0.37	0.52
$K_2(g/L)^{-1}$	10.00	10.00	10.00	10.00	10.00
$C_{min}(g/L)$	0.005	0.005	0.005	0.005	0.005
$V_o(m/h)$	13.00	12.00	14.00	6.40	9.00
MLSS(g/L)	2.52	2.98	2.10	2.01	2.96
$V_c(m/h)$	6.50	6.00	7.00	3.20	4.50
$K_c(g/L)^{-1}$	0.31	0.33	0.33	0.18	0.26
$Q_{in}(m^3/h)$	1764	828	2160	1368	792
$Q_r(m^3/h)$	1188	540	1152	792	432
SLR(kg/m^2-h)	5.21	2.85	4.87	3.04	2.54
RAS Ratio	0.67	0.65	0.53	0.58	0.55
SOR(m/h)	1.23	0.58	1.51	0.96	0.55
Returned Activated Sludge Concentration Predictions (g/L)					
Previous Experimental Results	5.420	6.700	5.780	5.280	8.760
2Dc Modeling Results (this study)	6.200	7.100	4.600	5.400	7.700
Effluent Suspended Solids Predictions (mg/L)					
Previous Experimental Results	13.50	7.80	10.50	12.80	11.30
2Dc Modeling Results (this study)	14.25	8.97	16.26	18.00	9.90

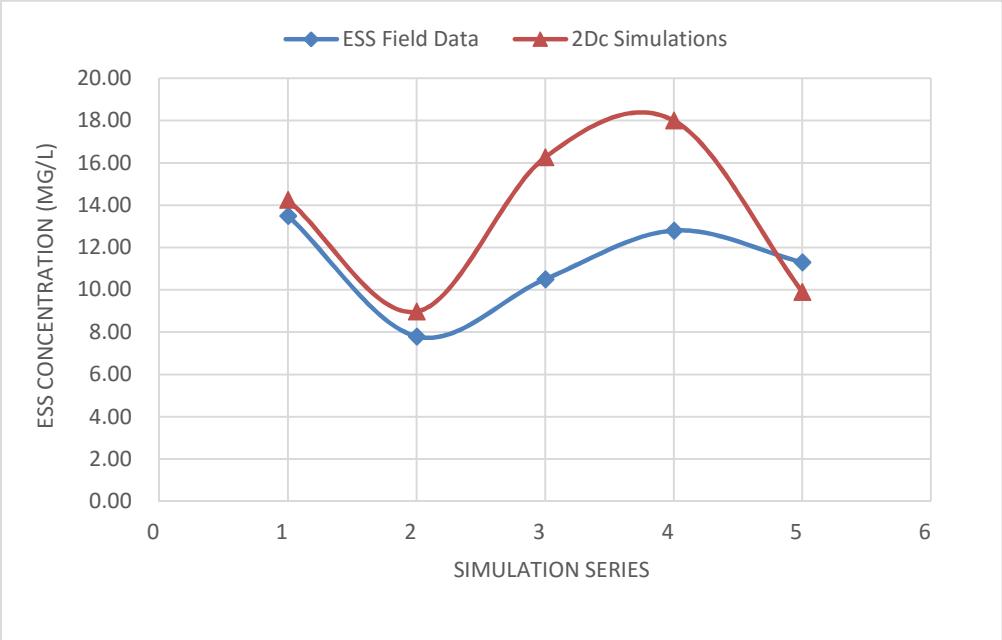

Figure 2. CFD Simulations Compared to Field Observations (Vitasovic, 1997).

Table 2 shows the performance of a secondary clarifier as the function of surface overflow rate (SOR) and solids loading rate (SLR) for K_1=0.62. Five simulations (simulations 6 to 10) are shown in the table. The comparisons of the modeling simulation are shown in the last six rows. Compared with the previous simulation of ESS, the 2Dc model is more stable and reliable. The simulation results of Table 2 are plotted in the Figure 8.

Table 2-Simulated effect of surface overflow rate and solids loading rate on effluent suspended solids, K_1=0.62 (Vitasovic et al., 1997) and results.

Simulations	6	7	8	9	10
$K_1(g/L)^{-1}$	0.62	0.62	0.62	0.62	0.62
$K_2(g/L)^{-1}$	10.00	10.00	10.00	10.00	10.00
C_{min}(g/L)	0.005	0.005	0.005	0.005	0.005
V_o (m/h)	13.00	13.00	13.00	13.00	13.00
MLSS(g/L)	2.52	2.52	2.52	2.52	2.52
V_c(m/h)	6.50	6.50	6.50	6.50	6.50
$K_c(g/L)^{-1}$	0.31	0.31	0.31	0.31	0.31
$Q_{in}(m^3/h)$	1000	1500	2000	2500	3000
$Q_r(m^3/h)$	600	900	1200	1500	1800
SLR(kg/m^2-h)	2.82	4.23	5.64	7.05	8.46
RAS Ratio	0.60	0.60	0.60	0.60	0.60
SOR(m/h)	0.70	1.05	1.40	1.75	2.09
Returned Activated Sludge Concentration Predictions (g/L)					
Previous Modeling Results	6.707	6.761	6.248	5.711	5.124
2Dc Modeling Results (this study)	6.600	6.620	6.610	6.590	6.550
Effluent Suspended Solids Predictions (mg/L)					
Previous Modeling Results	7.00	9.00	162.00	87.00	591.00
2Dc Modeling Results (this study)	9.50	12.84	15.80	19.89	**29.00**

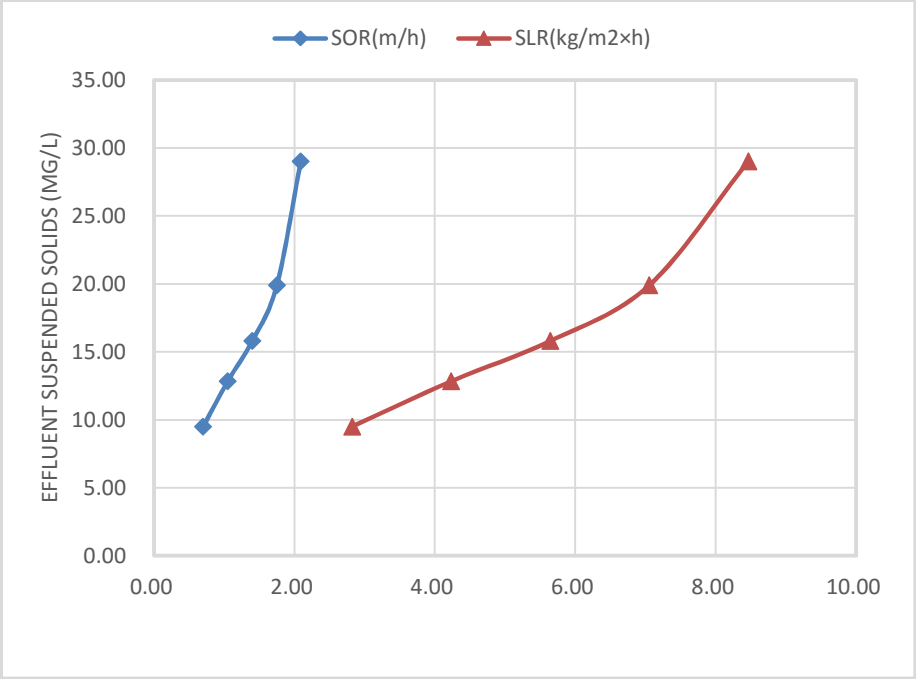

Figure 8-Predicted effluent suspended solids concentration as a function of surface overflow rate and solids loading rate shown in Table 2.

Similarly with Table 2, Table 3 shows the performance of secondary clarifier as the function of surface overflow rate (SOR) and solids loading rate (SLR) for lower K_1 (K_1=0.42). Five simulations (simulations 11 to 15) are shown in the table. The comparisons of the modeling simulation are shown in the last six rows. The simulation results of Table 3 are plotted in Figure 9. The simulation results in Tables 2 and 3, which are for different K_1, are compared in Figure 10.

Table 3-Simulated effect of surface overflow rate and solids loading rate on effluent suspended solids, K_1=0.42 (Vitasovic et al., 1997) and results.

Simulations	11	12	13	14	15
$K_1(g/L)^{-1}$	0.42	0.42	0.42	0.42	0.42
$K_2(g/L)^{-1}$	10.00	10.00	10.00	10.00	10.00
$C_{min}(g/L)$	0.005	0.005	0.005	0.005	0.005
V_o (m/h)	13.00	13.00	13.00	13.00	13.00
MLSS(g/L)	2.52	2.52	2.52	2.52	2.52
V_c(m/h)	6.50	6.50	6.50	6.50	6.50
$K_c(g/L)^{-1}$	0.21	0.21	0.21	0.21	0.21
$Q_{in}(m^3/h)$	1000	1500	2000	2500	3000
$Q_r(m^3/h)$	600	900	1200	1500	1800
SLR(kg/m^2-h)	2.82	4.23	5.64	7.05	8.46
RAS Ratio	0.60	0.60	0.60	0.60	0.60
SOR(m/h)	0.70	1.05	1.40	1.75	2.09
Returned Activated Sludge Concentration Predictions (g/L)					
Previous Modeling Results	6.704	6.711	6.695	6.641	6.507
2Dc Modeling Results (this study)	6.690	6.690	6.680	6.680	7.000
Effluent Suspended Solids Predictions (mg/L)					
Previous Modeling Results	6.00	9.00	15.00	26.00	62.00
2Dc Modeling Results (this study)	9.31	12.61	15.36	15.36	21.02

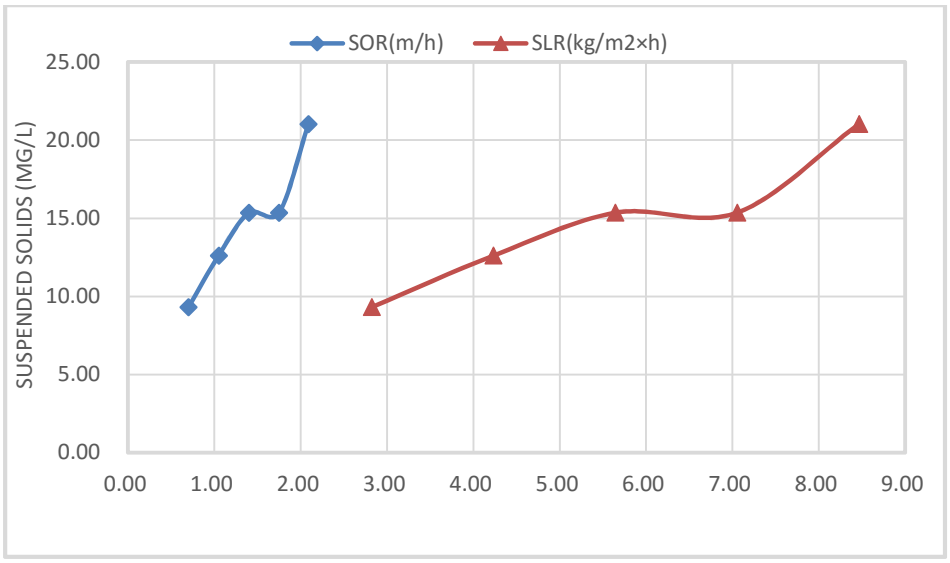

Figure 9-Predicted effluent suspended solids concentration as a function of surface overflow rate and solids loading rate for conditions shown in Table 3.

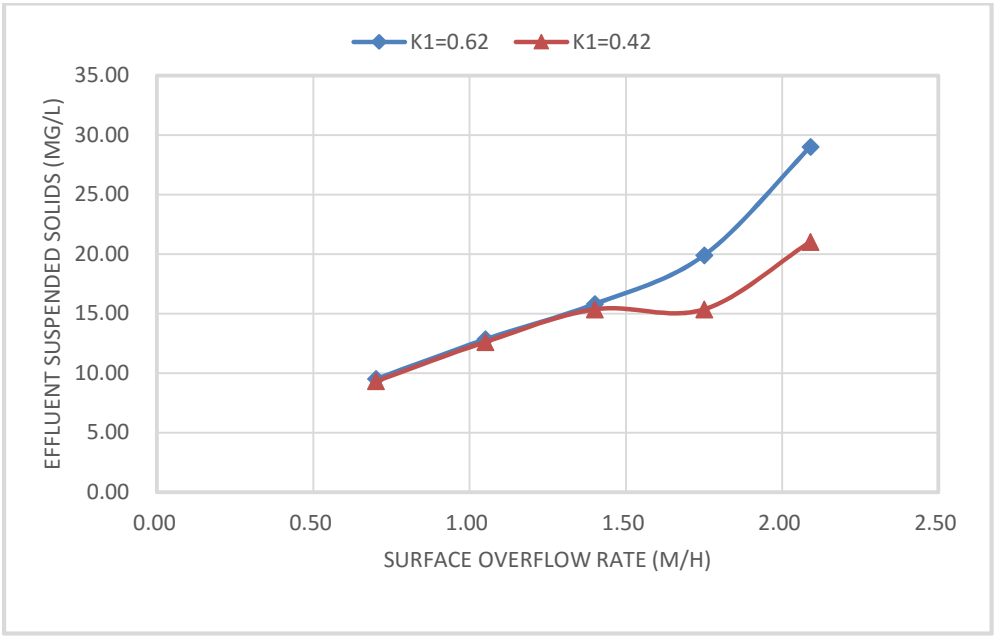

Figure 10- Predicted effluent suspended solids concentration as a function of settling parameter K_1 in Table 2, 3.

Table 4 shows the performance of secondary clarifier as the function of surface overflow rate (SOR) and solids loading rate (SLR) for lower MLSS (MLSS=1.8 g/L). Five simulations (simulations 16 to 20) are shown in the table. The comparisons of the modeling simulation are shown in the last six rows. The simulation results of Tables 2 and 4, which are for different MLSS, are plotted in Figure 11.

Table 4- Simulated effect of surface overflow rate and solids loading rate on effluent suspended solids at lower mixed liquor suspended solids, K_1=0.62 (Vitasovic et al., 1997) and results.

Simulations	16	17	18	19	20
$K_1(g/L)^{-1}$	0.62	0.62	0.62	0.62	0.62
$K_2(g/L)^{-1}$	10.00	10.00	10.00	10.00	10.00
$C_{min}(g/L)$	0.005	0.005	0.005	0.005	0.005
$V_o(m/h)$	13.00	13.00	13.00	13.00	13.00
MLSS(g/L)	1.80	1.80	1.80	1.80	1.80
$V_c(m/h)$	6.50	6.50	6.50	6.50	6.50
$K_c(g/L)^{-1}$	0.31	0.31	0.31	0.31	0.31
$Q_{in}(m^3/h)$	1000	1500	2000	2500	3000
$Q_r(m^3/h)$	600	900	1200	1500	1800
SLR(kg/m^2-h)	2.02	3.02	4.03	5.04	6.05
RAS Ratio	0.60	0.60	0.60	0.60	0.60
SOR(m/h)	0.70	1.05	1.40	1.75	2.09
Returned Activated Sludge Concentration Predictions (g/L)					
Previous Modeling Results	4.791	4.782	4.775	4.644	4.444
2Dc Modeling Results (this study)	4.780	4.770	4.770	4.760	4.760
Effluent Suspended Solids Predictions (mg/L)					
Previous Modeling Results	6.00	9.00	14.00	27.00	70.00
2Dc Modeling Results (this study)	9.11	12.46	15.42	18.48	21.46

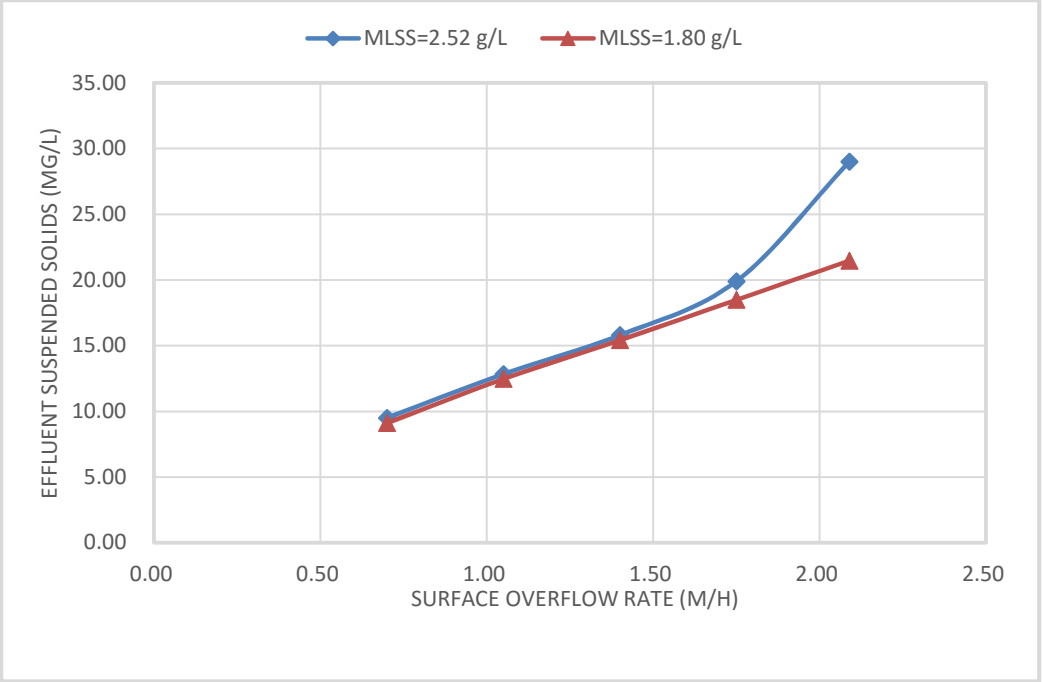

Figure 11-Predicted effluent suspended solids concentration as a function of MLSS in Tables 2 and 4.

Table 5 shows the performance of secondary clarifier as a function of the size of flocculating well. Twenty five simulations (simulations 6 to 10 and simulations 21 to 40) are shown in the table. The twenty five data sets are divided into five groups. The size of the flocculating well is fixed in each group, therefore, the trend of ESS for varied SORs can be observed in each group. In addition, the five groups show the change of performance as a function of the size of flocculating well; therefore, the change of ESS for different sizes of flocculating wells can be observed by comparing the ESS for the same SOR but different flocculation well size ratios. Since simulations 6 to 10 are simulated using the original size of the flocculating well, the results are included in Table 5 again to complete the comparison. The comparisons of the modeling simulation are shown in the last six rows. The simulation results of Table 5 are plotted in Figure 12.

Table 5- Predicted effluent suspended solids concentration as a function of geometry modifications.

K_1 $(g/L)^{-1}$	K_2 $(g/L)^{-1}$	Cmin (g/L)	Vo (m/h)	MLSS (g/L)	Vc (m/h)	Kc $(g/L)^{-1}$	RAS Ratio	peripheral baffle depth (m)
0.61	10.00	0.005	13.00	2.52	6.50	0.31	0.60	0.50
Simula -tions	radius of the flocculation well (m)	Ratio between the flocculation well diameter and total diameter	SOR, (m/h)	SLR, $(kg/m^2 \times h)$	Influe nt flow, (m^3/h)	RAS flow, (m^3/h)	RAS Conc (g/L)	ESS (mg/L)
21	5.978	28%	0.7	2.82	1000	600	6.61	14.09
22	5.978	28%	1.05	4.23	1500	900	6.58	20.67
23	5.978	28%	1.4	5.64	2000	1200	6.54	28.44
24	5.978	28%	1.75	7.05	2500	1500	6.48	38.36
25	5.978	28%	2.09	8.46	3000	1800	N/A	N/A
26	7.4725	35%	0.7	2.82	1000	600	6.64	12.43
27	7.4725	35%	1.05	4.23	1500	900	6.56	18.57
28	7.4725	35%	1.4	5.64	2000	1200	6.58	25.20
29	7.4725	35%	1.75	7.05	2500	1500	6.54	34.47
30	7.4725	35%	2.09	8.46	3000	1800	6.43	**54.02**
31	8.54	40%	0.7	2.82	1000	600	6.65	11.58
32	8.54	40%	1.05	4.23	1500	900	6.62	17.31
33	8.54	40%	1.4	5.64	2000	1200	6.58	22.68
34	8.54	40%	1.75	7.05	2500	1500	6.55	31.61
35	8.54	40%	2.09	8.46	3000	1800	6.47	**46.80**
6	9.75	46%	0.7	2.82	1000	600	6.60	9.50
7	9.75	46%	1.05	4.23	1500	900	6.62	12.81
8	9.75	46%	1.4	5.64	2000	1200	6.61	15.80
9	9.75	46%	1.75	7.05	2500	1500	6.59	19.89
10	9.75	46%	2.09	8.46	3000	1800	6.55	29.00
36	10.675	50%	0.7	2.82	1000	600	10.14	6.64
37	10.675	50%	1.05	4.23	1500	900	6.63	14.46
38	10.675	50%	1.4	5.64	2000	1200	6.59	18.35
39	10.675	50%	1.75	7.05	2500	1500	6.60	23.91
40	10.675	50%	2.09	8.46	3000	1800	6.53	39.44

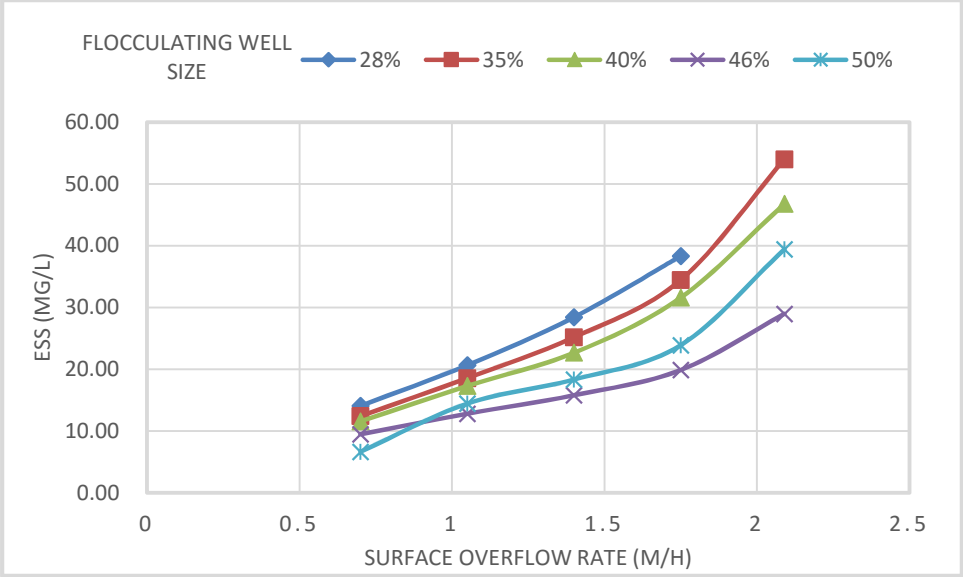

Figure 12- Effect of Surface Overflow Rate on Concentration of Effluent Suspended Solids for Different Size of Flocculating Well

Table 6 summarizes the influence of SOR and SLR on the performance of the SST. In matrix 1, simulations 41 through 56 are divided into four groups. The four groups have four different SLRs, but within each group the SLR is constant. The change of ESS can be observed with the increase of SOR in each group in Matrix 1. The change of ESS with the increase of SLR can be found by comparing the ESS with the same SOR but different SLR in different groups in the Matrix 1. In the Matrix 2, simulations 57 to 72 are also divided into four groups of data. Like the data in the Matrix 1, the first two groups of data in the matrix 2 (simulations 57 to 64) are obtained from the original paper, but the last two groups of data (simulations 65 to 72) are created in this study by averaging the SORs of the first two groups of data in the matrix 2 to have a better understanding of the influence of SOR on the performance of the SST. Differ with the Matrix 1, the four groups in the matrix 2 have different SORs, rather than SLRs, and they are

constant in the each group. Figures 13 and 14 show the ESS as a function of SOR and SLR based on the data in the two matrixes of Table 6.

Table 6-Summary of simulation and predicted effluent suspended solids concentrations as the function of surface overflow rate and solids loading rate (Wahlberg et al., 1998).

$K_1(g/L)^{-1}$	$K_2(g/L)^{-1}$	$C_{min}(g/L)$	$V_o(m/h)$	MLSS(g/L)	$V_c(m/h)$	$K_c(g/L)^{-1}$	
0.607	10.00	0.005	11.10	2.363	5.55	0.304	
Matrix 1	SOR (m/h)	SLR (kg/m^2-h)	Influent flow (m^3/h)	RAS flow (m^3/h)	RAS Ratio	RAS Conc (g/L)	ESS (mg/L)
41	0.35	2.04	503	729	1.45	6.64	10.14
42	0.52	2.04	746	486	0.65	5.84	8.63
43	0.61	2.04	869	364	0.42	7.48	9.24
44	0.66	2.04	842	292	0.35	8.32	9.63
45	0.53	3.05	757	1092	1.44	3.99	**9.39**
46	0.78	3.05	1120	729	0.65	5.94	11.14
47	0.91	3.05	1303	546	0.42	7.94	11.65
48	0.99	3.05	1412	437	0.31	9.89	12.20
49	0.37	4.07	524	1942	3.71	3.00	8.65
50	0.91	4.07	1301	1164	0.89	4.98	12.64
51	1.14	4.07	1634	831	0.51	6.79	14.55
52	1.27	4.07	1819	647	0.36	8.44	16.01
53	0.46	5.09	655	2428	3.71	3.00	9.48
54	1.14	5.09	1626	1456	0.90	4.96	14.84
55	1.43	5.09	2043	1039	0.51	NA	NA
56	1.59	5.09	2241	841	0.38	8.10	**21.80**

Matrix 2

57	0.46	1.34	655	158	0.24	9.45	7.88
58	0.46	2.05	655	584	0.89	4.96	8.21
59	0.46	3.17	655	1262	1.93	3.58	7.84
60	0.46	4.99	655	2366	3.61	3.01	9.46
61	1.14	3.57	1626	536	0.33	8.80	14.54
62	1.14	3.73	1626	631	0.39	8.07	14.51
63	1.14	4.77	1626	1262	0.78	5.33	14.72
64	1.14	5.89	1626	1940	1.19	4.33	14.94
65	0.70	2.05	1000	240	0.24	9.84	9.77
66	0.70	3.13	1000	890	0.89	4.99	10.64
67	0.70	4.85	1000	1930	1.93	3.58	11.25
68	0.70	7.63	1000	3610	3.61	3.01	11.55
69	0.90	2.64	1286	309	0.24	9.86	11.87
70	0.90	4.02	1286	1145	0.89	4.98	12.55
71	0.90	6.23	1286	2482	1.93	3.58	13.00
72	0.90	9.80	1286	4643	3.61	NA	NA

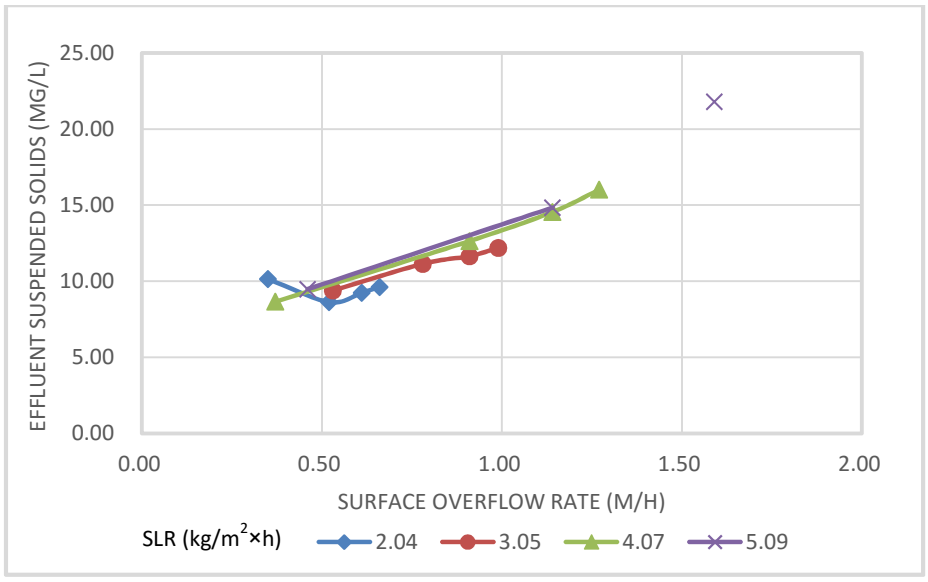

Figure 13 -Predicted effluent suspended solids concentration as a function of surface overflow rate for simulations 41 to 56 in Table 6.

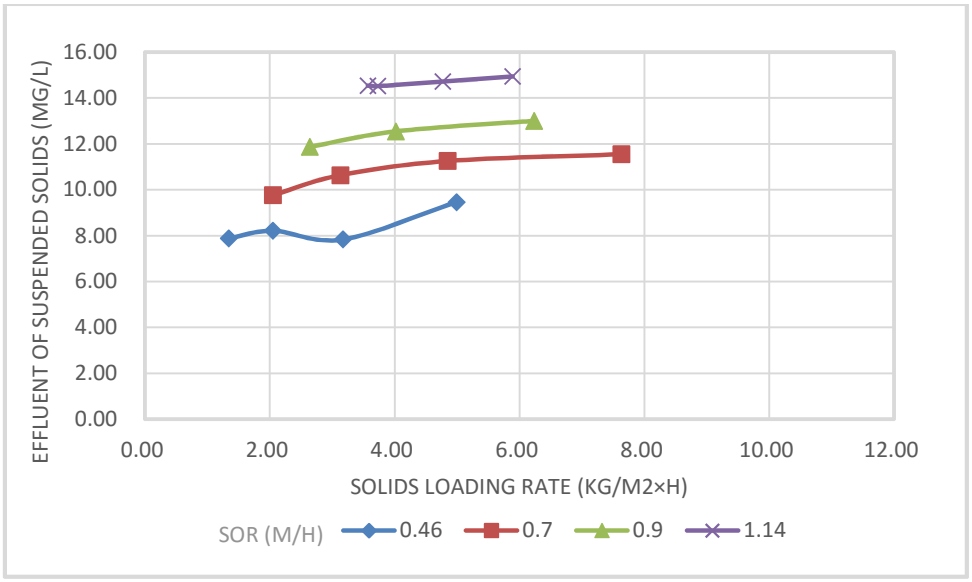

Figure 14-Predicted effluent suspended solids concentration as a function of solids loading rate for simulations 57 to 72 in Table 6.

4. Results and Discussion

4. 1. Effect of density currents on the performance of SSTs

Figures 3 to 7 present five flow patterns that are produced by performing simulations corresponding to the conditions from Table 1 defined as simulations 1 to 5. In Figures 4 and 7, the horizontal inflow does not reach the flocculating well, but turns sharply downward as a density waterfall. When this happens, the entrainment of low concentration fluids from the main settling zone flows back to the high concentration flocculating well and forms a strong recirculation eddy (Zhou et al., 1992). In the withdrawal zone, an eddy is formed by the bottom sludge reverse flow. Some researchers believe the density waterfall can deteriorate the performance of clarifiers by reducing the volume usage efficiency of flocculating well (Krebs, P., 1991; Vitasovic et al., 1997) and increasing the upward flow in the withdrawal zone corresponding to increase effluent suspended solid (Zhou et al., 1992). However, the simulations of simulations 2 and 5 show the formation of the density waterfall and the lowest ESS, compared with the results in simulations 1, 3 and 4. Tables 2 and 3 show the simulated conditions for two different settling parameters (K_1=0.62; K_1=0.42). After simulating the data in Tables 2 and 3, the same result is found from the solids distribution profiles, which the density waterfall is only formed in the first simulation of each table. The velocities and solids distribution and streamline for the first simulation in Tables 2 and 3 are shown in Figures 15a, b and 16a, b. The Figures 4b, 7b, 15b and 16b show that the density difference between the comparatively heavy fluid at the main settling zone and the relatively lighter fluid at the outlet zone causes a stable stratification. Samstag et al. (1992) revealed that the stable density stratification in the settling and effluent zone contributes to a significant damping of vertical mixing. Therefore, the density currents do

not bring about side effects on the ESS removal efficiency of the secondary clarifiers unless the upward currents can flow to the exit directly.

The Figures 4b, 7b, 15b and 16b are shown here due to their similar streamline.

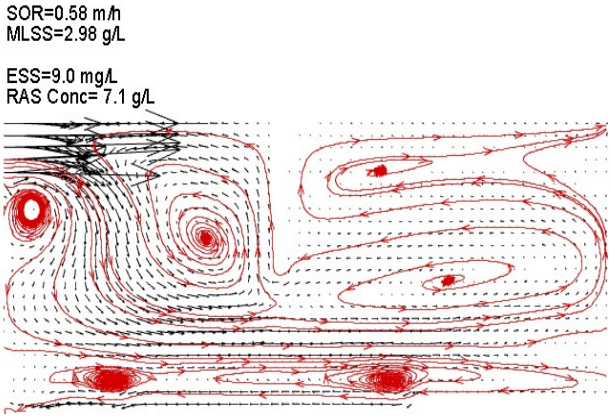

Figure 4(b) -Streamline for simulation 2.

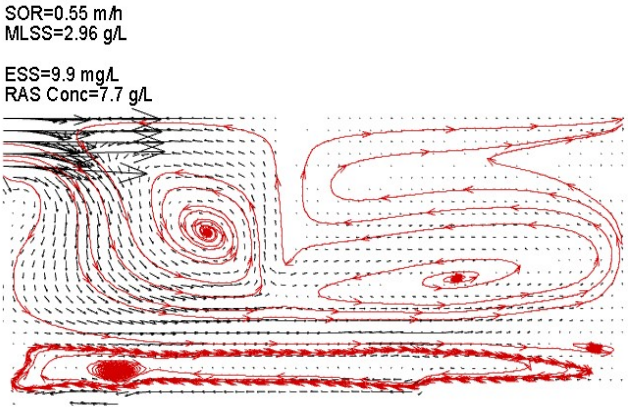

Figure 7(b) -Streamline for simulation 5.

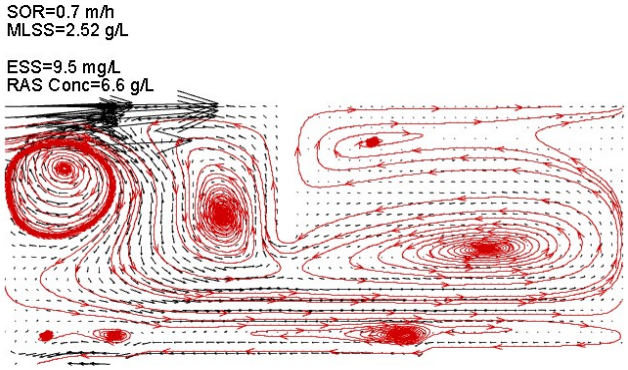

Figure 15 - (b) Streamline for simulation 6.

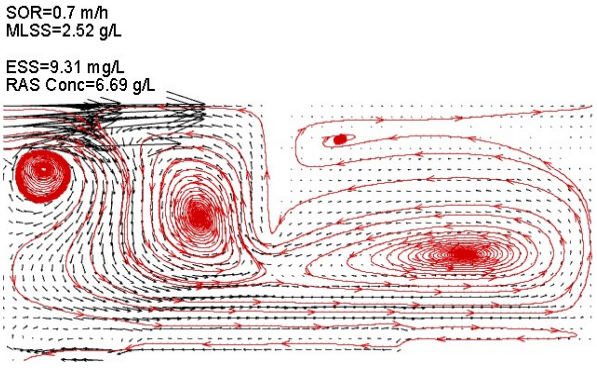

Figure 16 - (b) Streamline for simulation 11.

Figures 3b, 5b and 6b show differences from Figures 4b and 7b, indicating that the influent flow with higher SOR/SLR and lower MLSS concentration is deflected downward by impinging on the flocculating well. The downward flow splits to form an eddy inside the inlet zone and a forward bottom current in the settling zone.

The Figures 3b, 5b and 6b are shown here due to their similar streamline.

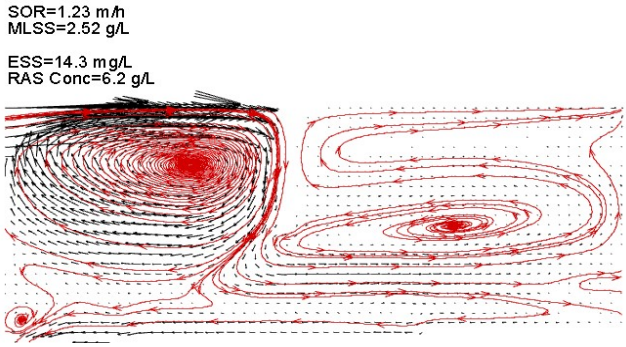

Figure 3 - (b) Streamline for simulation 1.

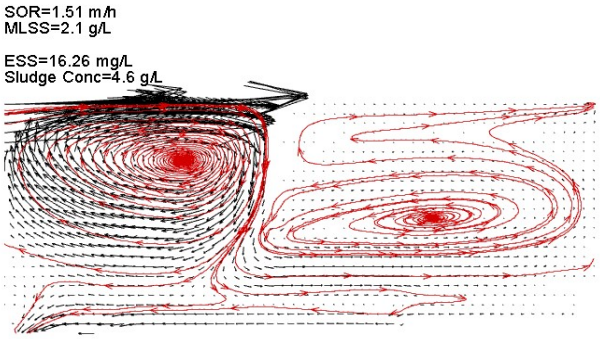

Figure 5 - (b) Streamline for simulation 3.

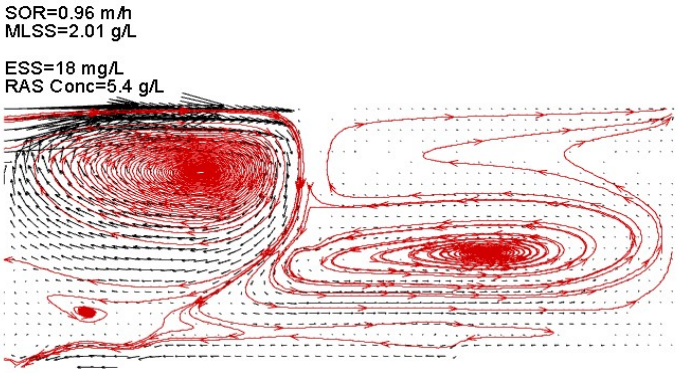

Figure 6 - (b) Streamline for simulation 4.

The similarity from Figures 3b to 7b illustrates that the currents in the withdrawal zone all the bottom currents flow counterclockwise towards to the flocculating well and then flow clockwise to the exit, instead of flowing upward to the effluent weir directly.

4. 2. Effect of Surface overflow rate (SOR) and Solids loading rate (SLR)

Vitasovic et al. (1997) used the data in the Tables 2 and 3 to study the influence of SOR and SLR on ESS. Based on Tables 2 and 3, the relationships between SOR, SLR and ESS are shown in Figures 8 and 9 already, and the ESS seems more sensitive with the variations of SOR than with SLR. However, since the SLR and SOR changed at the same time, it is better to keep one of the two parameters at a specific value and only change the left one. Hence, simulations 13

to 15 from Table 3 were selected and three new Tables (Tables 7a, b and c) were generated. Each table uses different SOR values with a specific SLR value. Figure 17 summarizes the outcomes of Tables 7a, b, and c.

Table 7a- Predicted effluent suspended solids concentration as a function of surface overflow rate based on simulation 13.

Simulations	73	74	13	75	76	77
$K_1(g/L)^{-1}$	0.42	0.42	0.42	0.42	0.42	0.42
$K_2(g/L)^{-1}$	10.00	10.00	10.00	10.00	10.00	10.00
$C_{min}(g/L)$	0.01	0.01	0.01	0.01	0.01	0.01
$V_o(m/h)$	13.00	13.00	13.00	13.00	13.00	13.00
MLSS(g/L)	2.52	2.52	2.52	2.52	2.52	2.52
$V_c(m/h)$	6.50	6.50	6.50	6.50	6.50	6.50
$K_c(g/L)^{-1}$	0.21	0.21	0.21	0.21	0.21	0.21
$Q_{in}(m^3/h)$	1500	1750	2000	2250	2500	2750
$Q_r(m^3/h)$	1700	1450	1200	950	700	550
SLR(kg/m^2-h)	5.64	5.64	5.64	5.64	5.64	5.64
ratio	1.13	0.83	0.60	0.42	0.28	0.20
SOR(m/h)	1.05	1.22	1.40	1.57	1.75	1.92
RAS Conc(g/L)	4.73	5.53	6.68	8.43	11.20	12.80
ESS(mg/L)	13.22	14.33	15.36	16.46	19.56	20.98

Table 7b- Predicted effluent suspended solids concentration as a function of surface overflow rate based on simulation 14.

Simulations	78	79	80	81	14	82
$K_1(g/L)^{-1}$	0.42	0.42	0.42	0.42	0.42	0.42
$K_2(g/L)^{-1}$	10.00	10.00	10.00	10.00	10.00	10.00
$C_{min}(g/L)$	0.01	0.01	0.01	0.01	0.01	0.01
$V_o(m/h)$	13.00	13.00	13.00	13.00	13.00	13.00
MLSS(g/L)	2.52	2.52	2.52	2.52	2.52	2.52
$V_c(m/h)$	6.50	6.50	6.50	6.50	6.50	6.50
$K_c(g/L)^{-1}$	0.21	0.21	0.21	0.21	0.21	0.21
$Q_{in}(m^3/h)$	1500	1750	2000	2250	2500	2750
$Q_r(m^3/h)$	2500	2250	2000	1750	1500	1250
SLR(kg/m^2-h)	7.05	7.05	7.05	7.05	7.05	7.05
ratio	1.67	1.29	1.00	0.78	0.60	0.45
SOR(m/h)	1.05	1.22	1.40	1.57	1.75	1.92
RAS Conc(g/L)	4.00	4.46	5.00	5.72	6.68	8.01
ESS(mg/L)	13.45	14.55	15.69	16.78	15.36	19.37

Table 7c- Predicted effluent suspended solids concentration as a function of surface overflow rate based on simulation 15.

Simulations	83	84	85	86	87	15
$K_1(g/L)^{-1}$	0.42	0.42	0.42	0.42	0.42	0.42
$K_2(g/L)^{-1}$	10.00	10.00	10.00	10.00	10.00	10.00
$C_{min}(g/L)$	0.01	0.01	0.01	0.01	0.01	0.01
$V_o(m/h)$	13.00	13.00	13.00	13.00	13.00	13.00
MLSS(g/L)	2.52	2.52	2.52	2.52	2.52	2.52
$V_c(m/h)$	6.50	6.50	6.50	6.50	6.50	6.50
$K_c(g/L)^{-1}$	0.21	0.21	0.21	0.21	0.21	0.21
$Q_{in}(m^3/h)$	1750	2000	2250	2500	2750	3000
$Q_r(m^3/h)$	3050	2800	2550	2300	2050	1800
SLR(kg/m^2-h)	8.46	8.46	8.46	8.46	8.46	8.46
ratio	1.74	1.40	1.13	0.92	0.75	0.60
SOR(m/h)	1.22	1.40	1.57	1.75	1.92	2.10
RAS Conc(g/L)	3.96	4.30	4.73	5.23	5.85	7.00
ESS(mg/L)	14.97	15.85	17.03	13.38	19.60	21.02

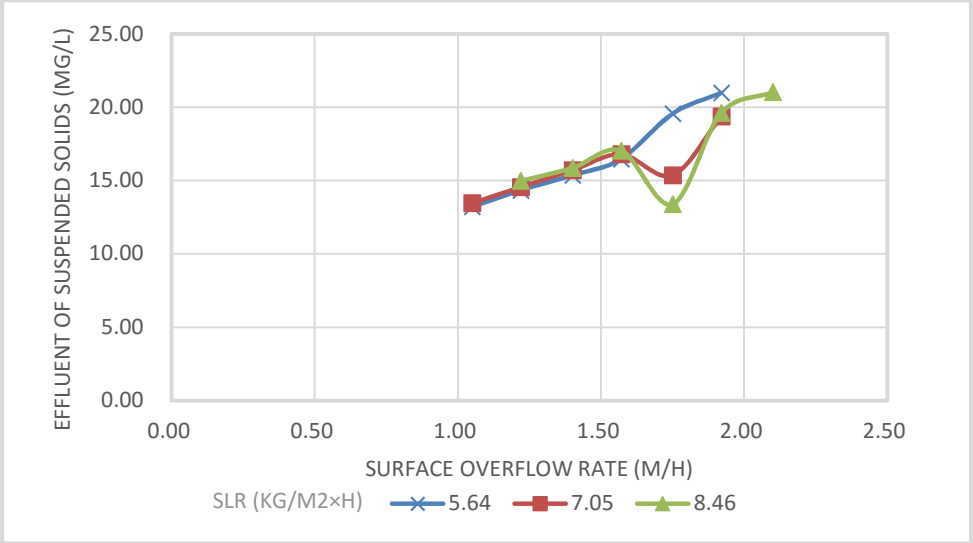

Figure 17- Predicted effluent suspended solids concentration as a function of surface overflow rate and solids loading rate for Table 7a, b, c

The data sets in the Figure 17 demonstrates that based on the 2Dc model, the SOR has a greater impact on ESS than the SLR. What is more, an interesting phenomenon is the ESS reaches to the minimum as the SOR increased to 1.57 m/h when the SLR=7.05 g/L and 8.46 g/L. Mccorquodale et al. (2004) explained that this may be caused by the improvement of hydrodynamics and the increase of flocculation process due to higher collision frequency of sludge particles.

In addition, the simulations based on the data set from the Wahlberg et al. (1998) are listed in Table 6. Figures 13 and 14 show the ESS as a function of SOR and SLR based on the data in the two matrixes of Table 6. The Figures 13 and 14 are already shown in Section 3 and are recaptured here.

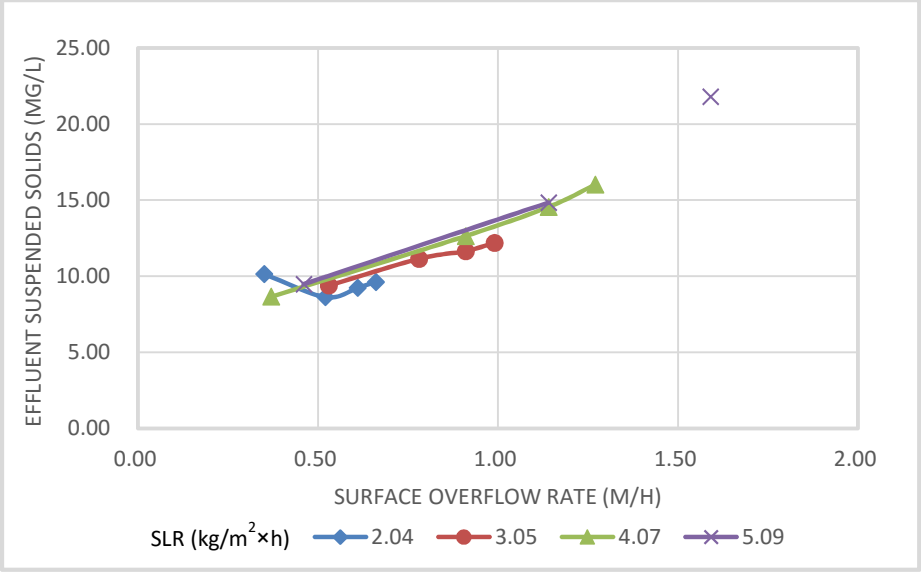

Figure 13 -Predicted effluent suspended solids concentration as a function of surface overflow rate for simulations 41 to 56 in Table 6.

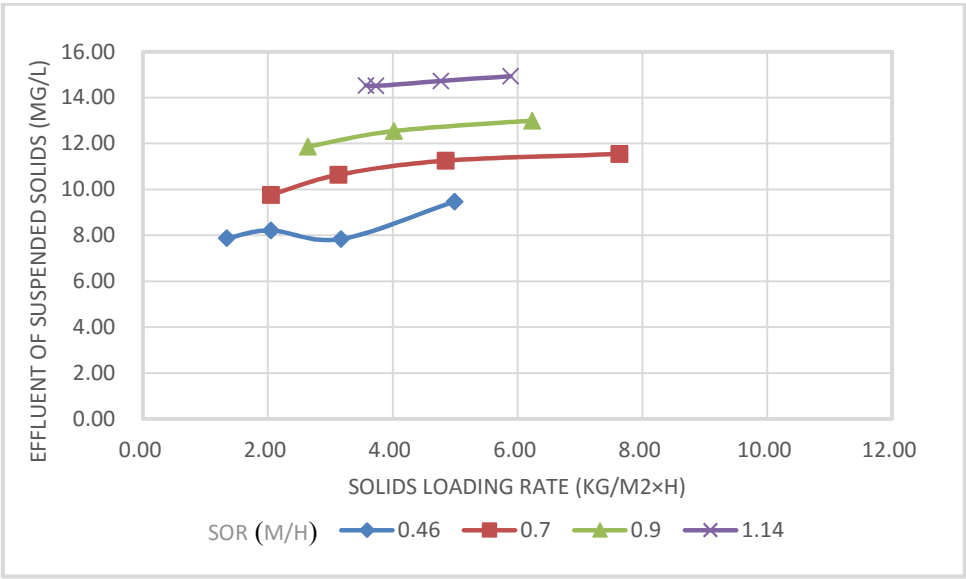

Figure 14-Predicted effluent suspended solids concentration as a function of solids loading rate for simulations 57 to 72 in Table 6.

The results reveal that the SOR that has greater contribution to ESS, which is opposite to Wahlberg et al.'s findings. There are three possible reasons for this contradiction.

Firstly, the disagreement may be caused by the differences of fundamental mathematical equations, such as continuity equation and turbulent equation, applied in the two models. In the 2Dc model, in order to include three dimensional effects, like swirl momentum and turbulence created by inlet and rotating scraper mechanisms, a third direction (θ direction) is included (McCorquodale et al., 2004). The governing equations of motion for three dimensional, incompressible, unsteady, stratified, incompressible, and turbulent- average flow in cylindrical coordinate (r, θ, y) in the 2Dc model are listed below (Jensen et al., 1979; McCorquodale et al., 2004):

Continuity equation

$$\frac{\partial ru}{\partial r} + \frac{\partial rv}{\partial y} + \frac{\partial r_{\ \theta}}{r\partial\theta} = 0$$

r -Momentum component:

$$\frac{\partial \rho u}{\partial t} + u\frac{\partial \rho u}{\partial r} + \frac{v_\theta}{r}\frac{\partial \rho u}{\partial \theta} - \frac{\rho v_\theta^2}{r} + v\frac{\partial \rho u}{\partial y} = -\frac{\partial p}{\partial r}$$
$$+\frac{1}{r}\frac{\partial}{\partial r}\left(r\mu_{eff}\frac{\partial u}{\partial r}\right) + \frac{1}{r^2}\frac{\partial}{\partial \theta}\left(\mu_{eff}\frac{\partial u}{\partial \theta}\right) - \frac{2}{r^2}\mu_{eff}\frac{\partial v_\theta}{\partial \theta} + \frac{\partial}{\partial y}\left(\mu_{eff}\frac{\partial u}{\partial y}\right) + \rho g_r$$

θ-Momentum component:

$$\frac{\partial \rho v_\theta}{\partial t} + u\frac{\partial \rho v_\theta}{\partial r} + \frac{v_\theta}{r}\frac{\partial \rho_{\ \theta}}{\partial \theta} + \frac{\rho v_\theta u}{r} + v\frac{\partial \rho_{\ \theta}}{\partial y}$$
$$= -\frac{1}{r}\frac{\partial p}{\partial \theta} + \frac{1}{r}\frac{\partial}{\partial r}\left(r\mu_{eff}\frac{\partial v_\theta}{\partial r}\right) + \frac{1}{r^2}\frac{\partial}{\partial \theta}\left(\mu_{eff}\frac{\partial v_\theta}{\partial \theta}\right) + \frac{1}{r^2}\mu_{eff}\frac{\partial u}{\partial \theta} + \frac{\partial}{\partial y}\left(\mu_{eff}\frac{\partial v_\theta}{\partial y}\right)$$
$$+ \rho g_\theta$$

y -Momentum component:

$$\frac{\partial \rho v}{\partial t} + u\frac{\partial \rho v}{\partial r} + \frac{v_\theta}{r}\frac{\partial \rho v}{\partial \theta} + v\frac{\partial \rho v}{\partial y}$$

$$= -\frac{\partial p}{\partial y} + \frac{1}{r}\frac{\partial}{\partial r}\left(r\mu_{eff}\frac{\partial v}{\partial r}\right) + \frac{1}{r^2}\frac{\partial}{\partial \theta}\left(\mu_{eff}\frac{\partial v}{\partial \theta}\right) + \frac{\partial}{\partial y}\left(\mu_{eff}\frac{\partial v}{\partial y}\right) + \rho\frac{\rho - \rho_r}{\rho}g_y$$

In which u, v, and v_θ are temporal mean velocity components in the r, θ, y directions respectively. μ_{eff} is the effective viscosity; p is the general pressure less the hydrostatic pressure at reference density ρ_r; ρ is the fluid-solid mixture density; g is the gravitational acceleration and ($\frac{\rho-\rho_r}{\rho_r}g_y$) is a density gradient term for the simulation of buoyant effects. In order to understand more details of the mathematical equations (e.g. solids transport equation, and turbulent equations) coupled in the 2Dc model, the readers are suggested to read McCorquodale et al. (2004).

For the comparison, the governing equations of motion for two-dimensional, unsteady, turbulent, and density stratified flow in the Vitasovic et al. (1997) are as follows:

Continuity equations:

$$\frac{\partial ru}{\partial r} + \frac{\partial rv}{\partial y} = 0$$

r -Momentum component:

$$\frac{\partial u}{\partial t} + u\frac{\partial u}{\partial r} + v\frac{\partial u}{\partial y} = -\frac{1}{\rho}\frac{\partial p}{\partial r} + \frac{1}{r}\frac{\partial}{\partial r}\left(r\vartheta_t\frac{\partial u}{\partial r}\right) + \frac{1}{r}\frac{\partial}{\partial y}\left(r\vartheta_t\frac{\partial u}{\partial y}\right) + S_u$$

y -Momentum component:

$$\frac{\partial v}{\partial t} + u\frac{\partial v}{\partial r} + v\frac{\partial v}{\partial y} = -\frac{1}{\rho}\frac{\partial p}{\partial y} + \frac{1}{r}\frac{\partial}{\partial r}\left(r\vartheta_t\frac{\partial v}{\partial r}\right) + \frac{1}{r}\frac{\partial}{\partial y}\left(r\vartheta_t\frac{\partial v}{\partial y}\right) - g\frac{\rho - \rho_r}{\rho} + S_v$$

where

$$S_u = \frac{1}{r}\frac{\partial}{\partial r}\left(r\vartheta_t\frac{\partial u}{\partial r}\right) + \frac{1}{r}\frac{\partial}{\partial y}\left(r\ _t\frac{\partial v}{\partial r}\right) - 2\frac{\vartheta_t}{r^2}u$$

and

$$S_v = \frac{1}{r}\frac{\partial}{\partial r}\left(r\vartheta_t \frac{\partial u}{\partial y}\right) + \frac{1}{r}\frac{\partial}{\partial y}\left(r\vartheta_t \frac{\partial v}{\partial y}\right)$$

All the same symbols shown in the two different references have the same mean, except ϑ_t shown in the Vitasovic et al. (1997) is eddy viscosity.

Secondly, the method used to analyze the relationship between these parameters might be a problem. The equation used for connect SLR, SOR and ESS is

SLR=SOR × (1+RAS Ratio) × MLSS.

Usually the relationship between these three parameters is just simply studied by keeping one of the SLR and SOR constant to study the effect of another parameter on ESS. However, we cannot ignore the impact of RAS ratio on the performance of clarifier. For example, the SOR and ESS is usually studied by keeping SLR and MLSS constant. However, as the SOR increases, the RAS ratio will decrease. Both changes of the two parameters will cause negative effect on the ESS concentration of the SST. At the same time, the increase of RAS ratio will reduce the MLSS concentration in the aeration tank. In another case, in order to study the SLR and ESS, usually the SOR and MLSS will be kept constant. Therefore, the RAS ratio will rise as the increase of SLR. As a result, the impact of rising the RAS ratio will offset the negative contribution of the SLR on the ESS. Also, increasing the RAS ratio will increase the concentration of MLSS flowing to the SST. Therefore, the study of the SOR/SLR on ESS of secondary clarifier by keeping MLSS concentration and one of the SOR/SLR constant is problematic and other methods are needed to illustrate the relationship between the parameters.

Thirdly, Wahlberg et al (1993) explains that there is no relationship between SOR, SLR and ESS when the secondary clarifier is well designed and well operated. Therefore, he believes it is meaningless to study the relationship between SOR, SLR and ESS.

4. 3. Effect of solids-settling characteristics

The property of solids-settling, which is described by settling parameter K_1, has been reported to be one of the most important variables affecting the performance of clarifier because of the strong effect on the thickening ability (Vitasovic et al., 1997). The relationship between K_1 and SSVI (Settled Sludge Volume Index) was given by the empirical formula in Daigger (1995):

$$K_1 = 0.0583 + 0.00405 \times SSVI$$

Using Daigger's equation, a SSVI of 139 yields K_1=0.62, and a SSVI of 90 gives an equivalent of K_1=0.42. The high value of SSVI (or K_1) indicates poor settling and may cause clarifier failure (Vitasovic et al., 1997). The author shows the effect of K_1 on the sludge blanket level can be examined by comparing the figures of simulations 1, 2, 3 with simulation 4 in the paper, which the sludge blanket level in the first three cases is much higher than that in simulation 4. However, the results of the 2Dc model show that the relationship between K_1 and sludge blanket level cannot be identified from simulations 1 to 5. The simulation 3 and 4 show the similar sludge blanket depth, but K_1 of simulation 4 is almost the twice as much as the K_1 of simulation 3. The results show that the sludge blanket depth can be influenced by other parameters, such as settling velocity, concentration of MLSS, SOR etc. Hence, other influential factors need to be kept the same when studying the K_1. The best settling can be found in Figures

4a and 7a, compared with Figures 3a, 5a and 6a. This is consistent with the concentration of the ESS of simulations 2 and 5, which are comparatively lower than simulations 1, 3 and 4.

The Figures 4a and 7a are shown here due to their good settling performance.

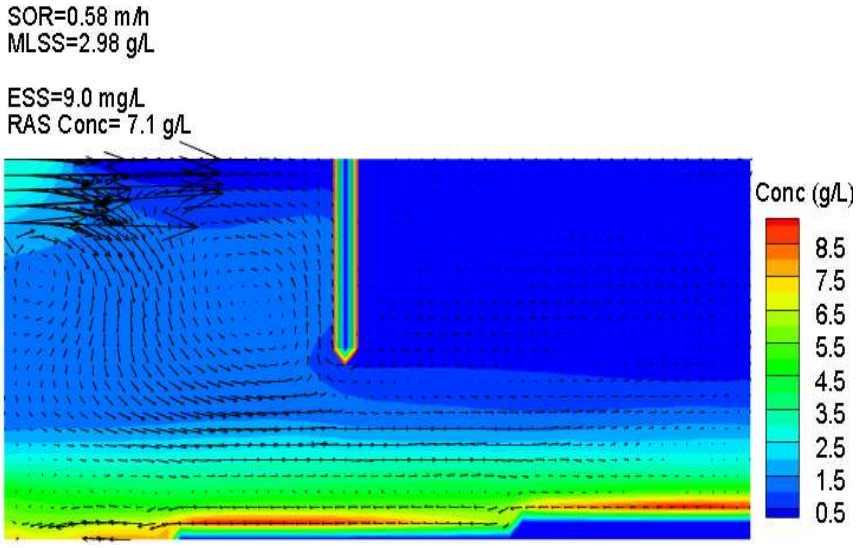

Figure 4a - Velocities and solids distribution for simulation 2.

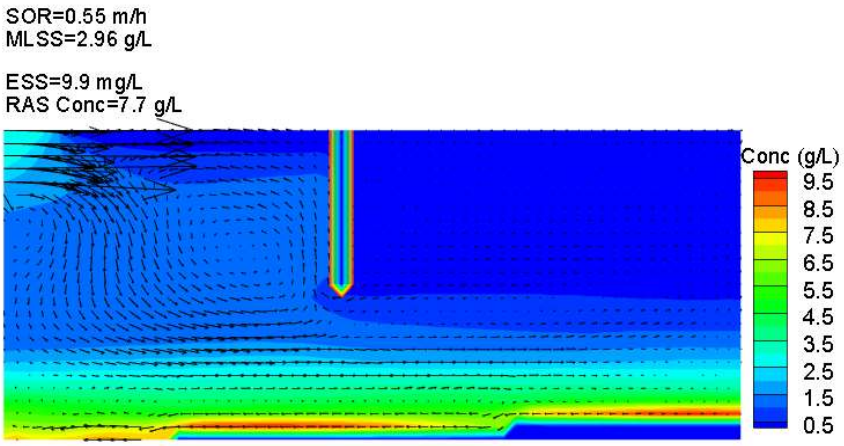

Figure 7a- Velocities and solids distribution for simulation 5.

The Figures 3a, 5a and 6a are shown here due to their similar settling performance.

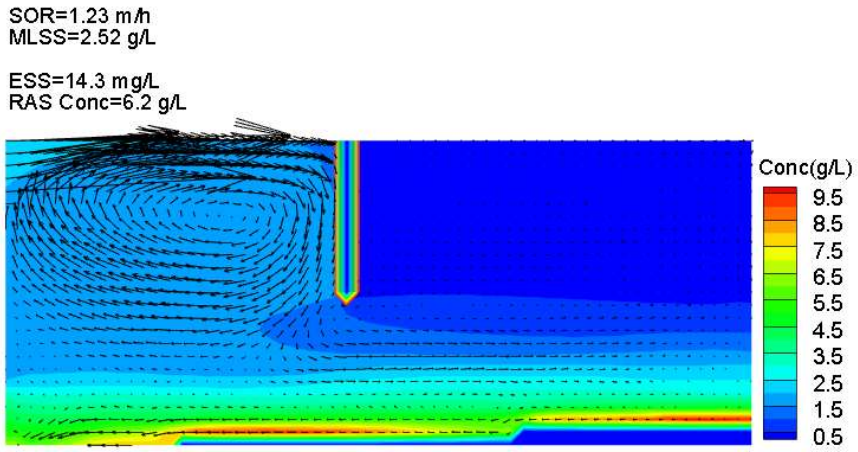

Figure 3a - Velocities and solids distribution for simulation 1.

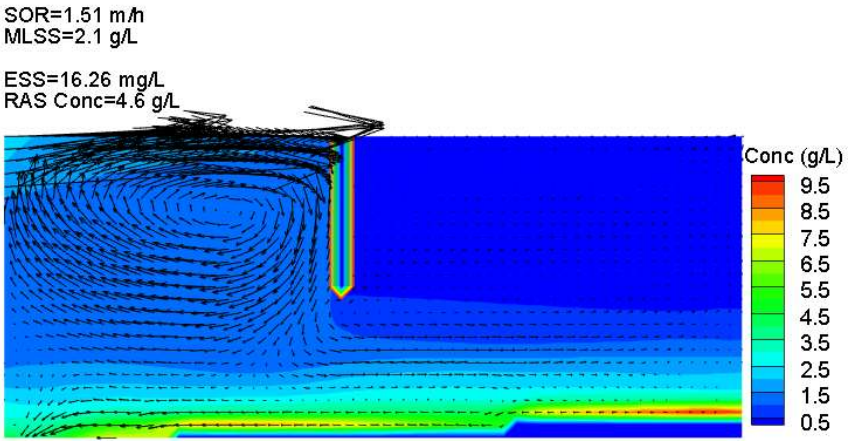

Figure 5a - Velocities and solids distribution for simulation 3.

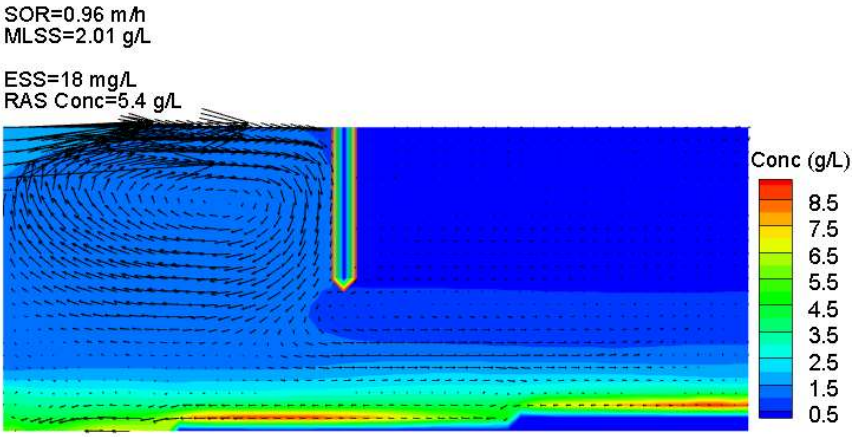

Figure 6a - Velocities and solids distribution for simulation 4.

The effect of K_1 on the ESS can be examined by comparing simulations in Tables 2 and 3. The results are shown in Figure 10 and recapture here.

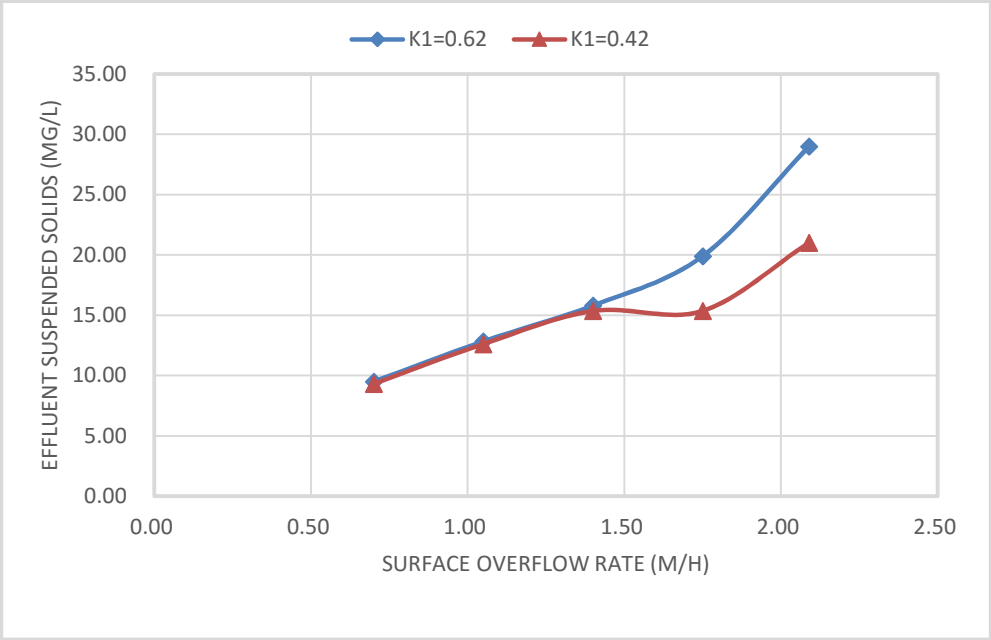

Figure 10- Predicted effluent suspended solids concentration as a function of settling parameter K_1 in Table 2, 3.

It shows that as the SOR increase, a lower K_1 produces a lower ESS concentration. However, compared with the data in the Vitasovic et al. (1997), the improvement to the effluent quality is insignificant.

4. 4. Effect of different MLSS values on ESS

Another important operation parameter of clarifier is the influent MLSS concentration (Vitasovic et al., 1997). To determine the effect of MLSS, the conditions described in Table 4 are simulated across a range of SORs with lower MLSS values. In Figure 11, the data show a similar conclusion to the effect of settling parameter (K_1). The effect of lower MLSS from 2.52 g/L to 1.80 g/L is not obvious, compared with the results in the paper. The outcomes of the 2Dc model

indicate that lower MLSS still reduce slightly on the ESS for the last two cases with higher SORs. Figures 18a, b show the velocities and solids distribution for the first case in Table 4. Comparison of the flocculating zone for two different MLSS concentrations in Figures 15 and Figure 18 shows that two well-developed eddice are observed in the flocculating well in Figure 15. The higher MLSS (Figure 15) is due to the decline of the strong eddy below the inlet, because the density gravity force is dominant compared to the initial momentum. At the same time, reducing the eddy below the inlet contributes to the enlargement of the eddy near the flocculating well.

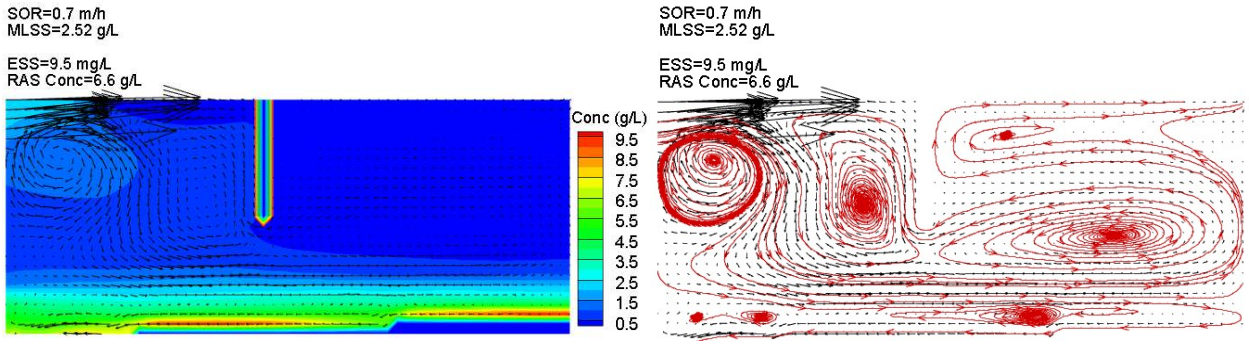

Figure 15-(a) Velocities and solids distribution and (b) streamline for simulation 6 in Table 2.

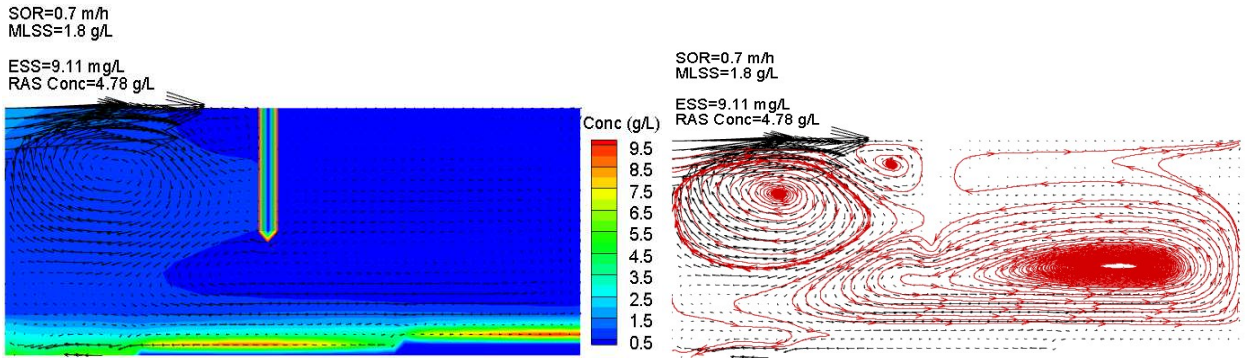

Figure 18-(a) Velocities and solids distribution and (b) streamline for simulation 16 in Table 4.

4. 5. Effect of the size of flocculating well and the peripheral baffle on the SS removal efficiency of the SST.

To exemplify the effect of tank design on the performance of the tank, a modification in clarifier geometry is simulated for different SOR values. All the other inputs (size alteration of flocculating well, peripheral baffle size and location, K_1, Stokes velocity, MLSS and RAS ratio) are equal to the values in the Vitasovic et al. (1997). Outputs shown in Table 5 indicate that after adjusting the size of the flocculating well from 46% to 28% of the tank diameter, the modified tank produces even higher ESS. Solids and velocity patterns for the unmodified and modified tanks are shown from Figures 19a to 23a and Figures 24a to 27a, respectively. The simulation of the last test for the 28% of tank diameter modification cannot be simulated by the 2Dc model, so there are only four results for the 28% of tank diameter modification. The figures of both modified and unmodified tanks show that the rise of sludge blanket interface will ultimately contributes to the break of limitation of ESS concentration. For the retrofitted tank, the break comes out even earlier than the original tank. The streamline profiles for the unmodified and modified tanks are shown from Figures 19b to 23b and Figures 24b to 27b, respectively. Figures 19 to 27 are listed in the Appendix. The comparisons for streamline profiles in both of the tanks display a same trend: when the SLR increases with SOR at a constant RAS ratio, the strong eddy in the main settling zone becomes smaller and finally disappears. The currents, which were found to form the eddy, flow out directly from the end of the flocculating well lip.

Later on, in order to convince the modeling results, addition simulations were performed at 35%, 40% and 50% of the tank diameter. The results of these modifications are shown in Table 5 and Figure 12.

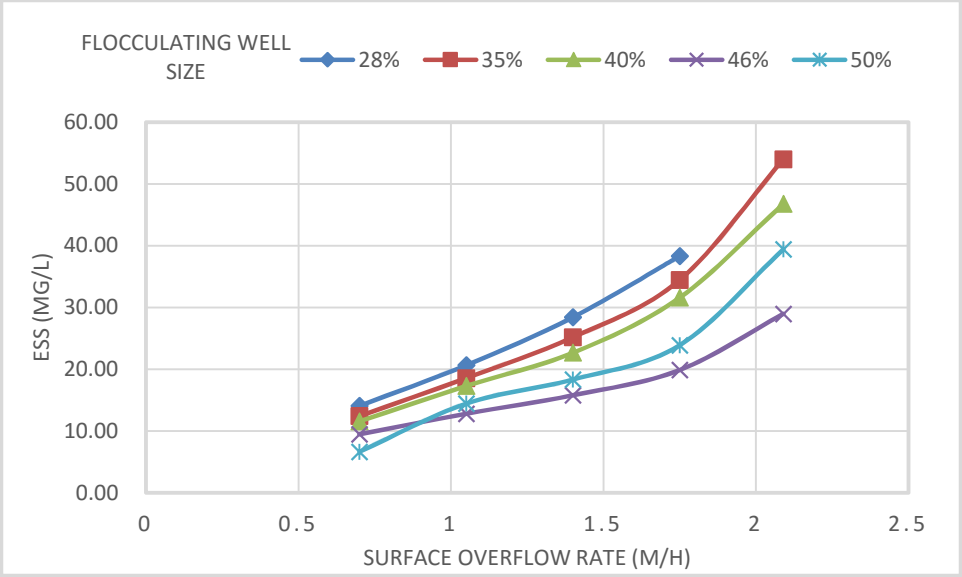

Figure 12- Effect of Surface Overflow Rate on Concentration of Effluent Suspended Solids for Different Size of Flocculating Well.

Figure 12 shows that the smaller flocculating well produces higher ESS. Although this outcome is opposite to the result of the simulation provided by Vitasovic et al. (1997), it is consistent with the conclusion of Parker et al. (1971) that larger flocculation wells usually create better flocculation condition and less ESS. The simulations demonstrate that the optimal size of the flocculating well is 46% of the tank diameter, which is the original size of the well. This may be the reason why the effect of reducing of MLSS concentration from 2.52 to 1.80 g/L and changing the K_1 from 0.62 to 0.42 L/g is small compared with the conclusions in the Vitasovic et al. (1997). The conclusions of the literature illustrate that changing the value of MLSS and settling parameter K_1 may decrease the ESS concentration when the geometry of the tank is not optimal.

In addition, the comparison of the last simulation (simulations 25, 30 and 35), each of the flocculating well size shows that equilibrium cannot be reached after 400 minutes of steady input

when the size of the flocculating well is comparatively small. Therefore, simulations with larger flocculating well achieves equilibrium earlier in ESS and may improve numerical accuracy.

To illustrate the impact of adding a peripheral baffle on the performance of the secondary clarifier, two additional groups of simulations with different baffle height were performed for the condition of simulations 10 (did not reach equilibrium) and 20 (reach equilibrium). The results are shown in Table 8, Figures 28 and 29.

Table 8- Simulated effect of depth of peripheral baffle on effluent suspended solids and results

Simu la-tions	K_1 $(g/L)^{-1}$	K_2 $(g/L)^{-1}$	C_{min} (g/L)	V_o (m/h)	MLSS (g/L)	V_c (m/h)	Kc $(g/L)^{-1}$	Q_{in} (m^3/h)	Q_r (m^3/h)	SLR (kg/m^2-h)	RAS Ratio	SOR (m/h)	depth (m)	RAS Conc (g/L)	ESS (mg/L)
10	0.62	10	0.005	13	2.52	6.50	0.31	3000	1800	8.46	0.6	2.09	\	6.55	29.00
73	0.62	10	0.005	13	2.52	6.50	0.31	3000	1800	8.46	0.6	2.09	0.3	6.53	44.21
74	0.62	10	0.005	13	2.52	6.50	0.31	3000	1800	8.46	0.6	2.09	0.4	6.53	44.21
75	0.62	10	0.005	13	2.52	6.50	0.31	3000	1800	8.46	0.6	2.09	0.5	6.51	42.66
76	0.62	10	0.005	13	2.52	6.50	0.31	3000	1800	8.46	0.6	2.09	0.9	6.48	39.07
77	0.62	10	0.005	13	2.52	6.50	0.31	3000	1800	8.46	0.6	2.09	1	6.48	39.07
78	0.62	10	0.005	13	2.52	6.50	0.31	3000	1800	8.46	0.6	2.09	1.1	6.65	52.81
20	0.62	10	0.005	13	1.80	6.50	0.31	3000	1800	8.46	0.6	2.09	\	4.76	21.46
79	0.62	10	0.005	13	1.80	6.50	0.31	3000	1800	8.46	0.6	2.09	0.3	4.77	26.08
80	0.62	10	0.005	13	1.80	6.50	0.31	3000	1800	8.46	0.6	2.09	0.5	4.77	26.08
81	0.62	10	0.005	13	1.80	6.50	0.31	3000	1800	8.46	0.6	2.09	0.7	4.74	28.43
82	0.62	10	0.005	13	1.80	6.50	0.31	3000	1800	8.46	0.6	2.09	1	4.75	22.66
83	0.62	10	0.005	13	1.80	6.50	0.31	3000	1800	8.46	0.6	2.09	1.3	4.75	21.12
84	0.62	10	0.005	13	1.80	6.50	0.31	3000	1800	8.46	0.6	2.09	1.6	4.76	20.89
85	0.62	10	0.005	13	1.80	6.50	0.31	3000	1800	8.46	0.6	2.09	1.9	4.76	20.89
86	0.62	10	0.005	13	1.80	6.50	0.31	3000	1800	8.46	0.6	2.09	2.2	4.77	18.77
87	0.62	10	0.005	13	1.80	6.50	0.31	3000	1800	8.46	0.6	2.09	2.4	4.76	17.22
88	0.62	10	0.005	13	1.80	6.50	0.31	3000	1800	8.46	0.6	2.09	2.6	4.77	19.20
89	0.62	10	0.005	13	1.80	6.50	0.31	3000	1800	8.46	0.6	2.09	2.8	4.75	21.06

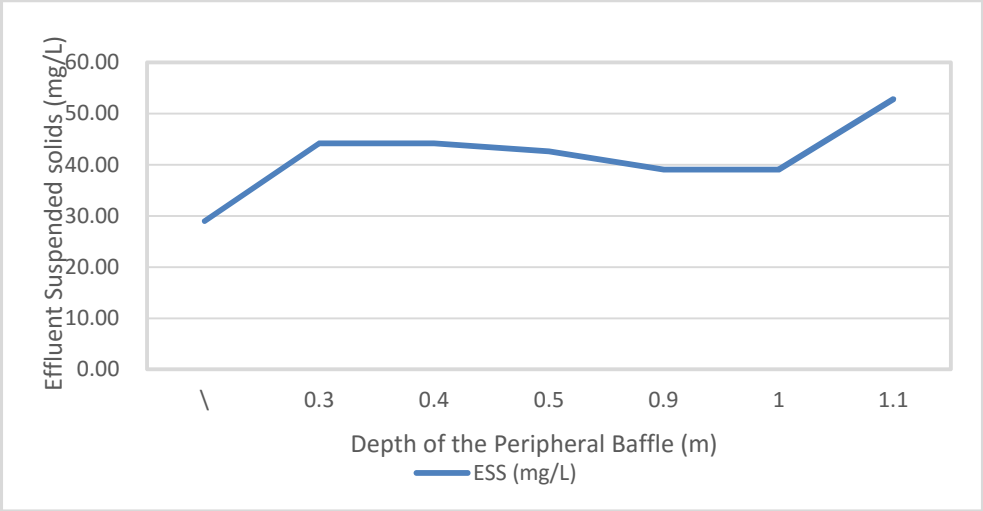

Figure 28- Effect of Depth of Peripheral Baffle on Effluent Suspended Solids for simulation 10.

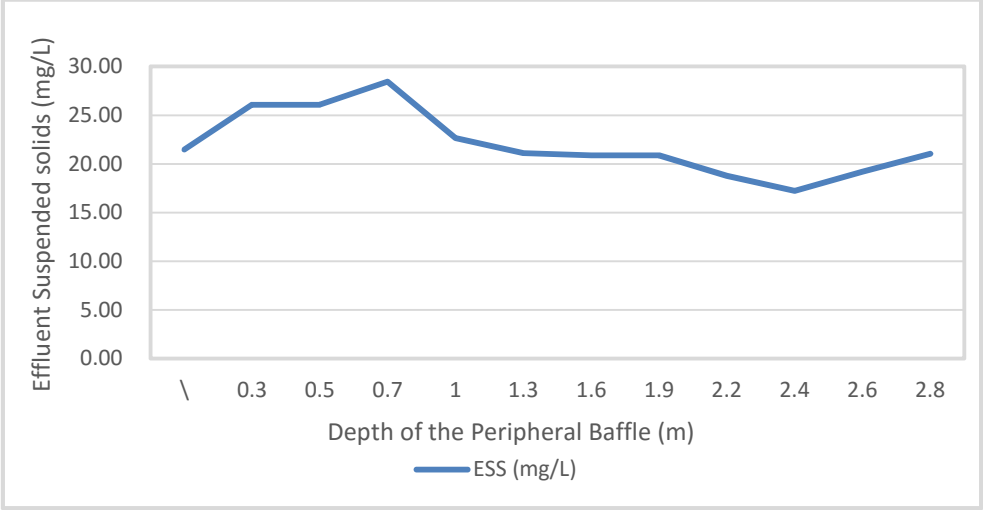

Figure 29- Effect of Depth of Peripheral Baffle on Effluent Suspended Solids for simulation 20.

Figure 28 shows when the ESS does not reach the equilibrium, adding the peripheral baffle can deteriorate the effluent quality. Conversely, Figure 29 indicates when the clarifier is for the steady state, adding the baffle can improve the effluent quality. On the one hand, when the baffle is less than 1 meter to the surface of the water, the ESS increases. One assumption is that

the close distance between the peripheral baffle and the top of the effluent weir restricts effluent flow passing through the section and creates very strong flow intensity around the effluent area. In addition, when the depth is more than 1 meter, which is approximately 1.9 meters to the top of the sludge blanket, the ESS decrease. The optimal depth of the peripheral baffle is 2.4 meters to the top of the effluent, which is about 0.9 meter to the top of the sludge blanket. This is accordant with Chu et al., (2015), which illustrates the distance between Stamford baffle and the surface of the sludge blanket is typically 3 to 5 feet.

5. Conclusions

This thesis has evaluated the concepts of using a mechanic clarifier model to secondary clarifier performance. A more advanced model (Q3D) was compared to an elder, less advanced model (2D) which does not include swirl velocity. There are a number of differences in the results which are as follows:

Application of a mechanistic clarifier model and using the data from the literature, the following conclusions are made:

1. There are some differences between the model predictions made by the Quasi 3-D (Q3D) axisymmetric model package and the 2-D model developed by Vitasovic et al (1997). This might be caused by the deviations of mathematical equations, such as continuity equation and turbulent equation, applied in the two models. The Q3D model is more powerful and accurate, considering its inclusion of three dimensional effects, such as like swirl momentum and the more precise description of viscosity.

2. Simulation results confirm the existence of density waterfall in the cases with low flow rate and high MLSS (as shown in simulations 2 and 5). However, the data do not show the side effect of density currents on the clarifier removal efficiency, because stable stratification in the main settling and outlet zones resists the upward dispersion of suspended solids. The bottom currents in the withdrawal zone, instead of flowing upward to the effluent weir directly, flow counterclockwise towards to the flocculating well and then flow clockwise to the exit. Therefore, the density waterfall does not deteriorate the hydraulic efficiency if stable stratification is existed in the main settling zone and effluent zone.

3. The results of the Q3D numerical model reveal that the impact of surface overflow rate (SOR) on effluent suspended solid (ESS) is more significant than solids loading rate (SLR). This is opposite to the simulation results in the Vitasovic et al (1997). The analyses were arranged to evaluate the different impacts of SOR and SLR on ESS using the relationship SLR=SOR×(1+RAS ratio)×MLSS. Different results may be possible if the MLSS was varied independently of SOR or SLR, and this is a topic for future, additional research.

4. The effect of changing the settling parameter K_1 0.42 to 0.62 L/g and adjusting the MLSS concentration from 2.52 to 1.80 g/L on the performance of secondary settling tank is insignificant when the geometry has been optimized.

5. The simulation results show that increasing the flocculating well size from 28% to 50% of the tank diameter resulted in lower ESS concentration. At smaller well sizes, the simulation took much longer to reach equilibrium, suggesting that there may be some uncertainty in the numerical method for these conditions that merits future work.

6. The addition of a peripheral baffle reduced ESS at steady-state and at steady-state, an optimal baffle height exists, which is approximately one to two meters above the sludge blanket surface. If routine operation requires deep sludge blankets, a shallow baffle is preferred.

7. A numerical model can be used to predict or verify the hydraulic efficiency of the clarifier. The present model package is capable of solving complex analysis of clarifier for different operating and design conditions, such as influent flow rate, inlet solids concentration, flocculation, temperature, settling property, internal clarifier geometry (for example, energy dissipating baffle, flocculation well, and withdrawal arrangements).

6. Appendix Figures.

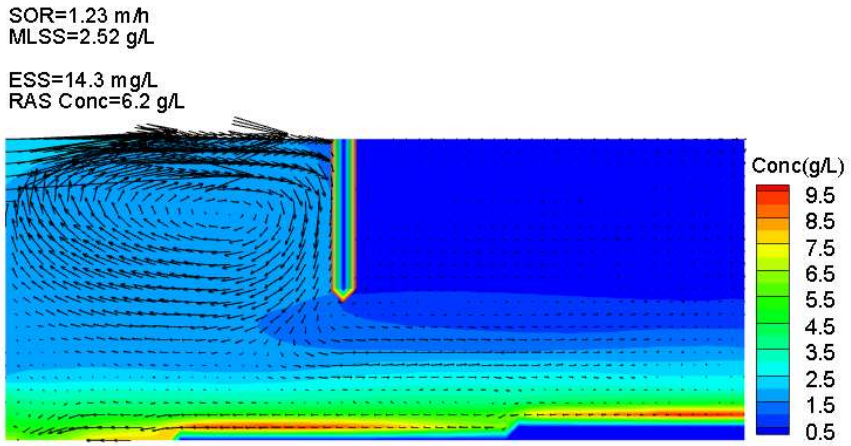

Figure 3- (a) Simulated velocities and solids distribution (Simulation 1).

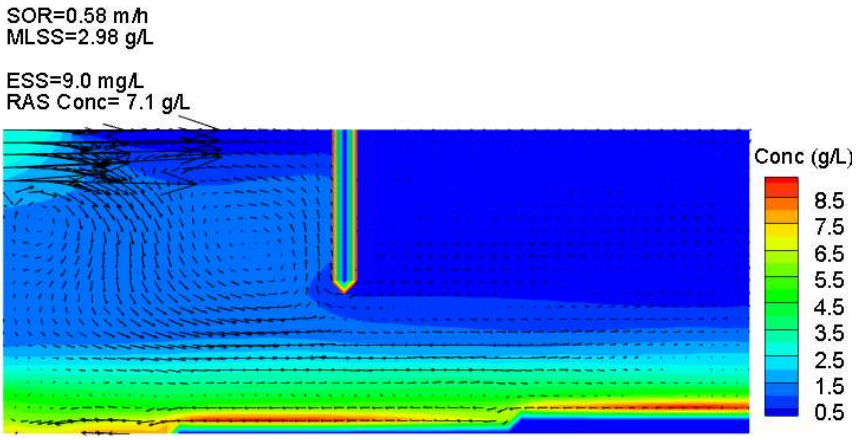

Figure 4- (a) Simulated velocities and solids distribution (Simulation 2).

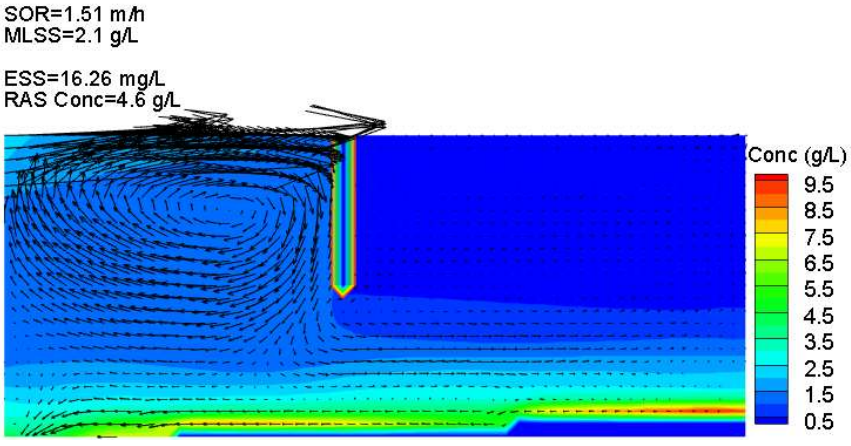

Figure 5- (a) Simulated velocities and solids distribution (Simulation 3).

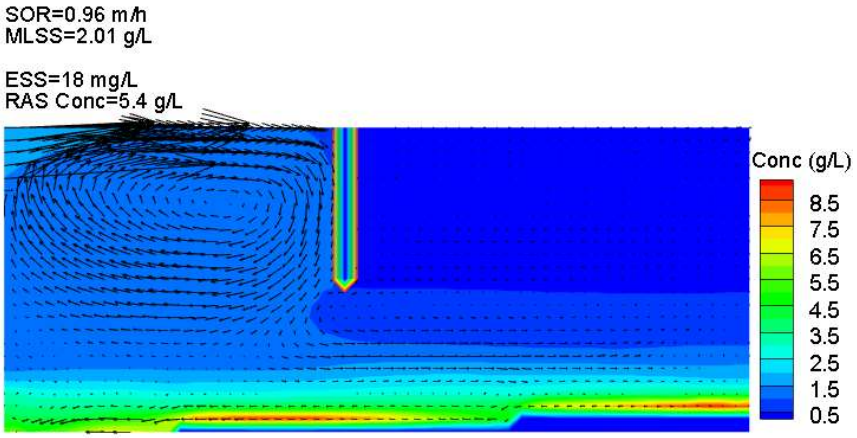

Figure 6 (a) Simulated velocities and solids distribution (Simulation 4).

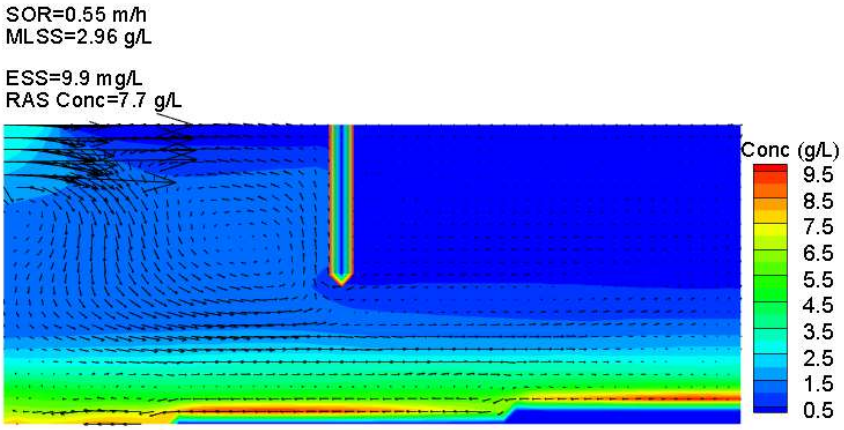

Figure 7- (a) Simulated velocities and solids distribution (Simulation 5).

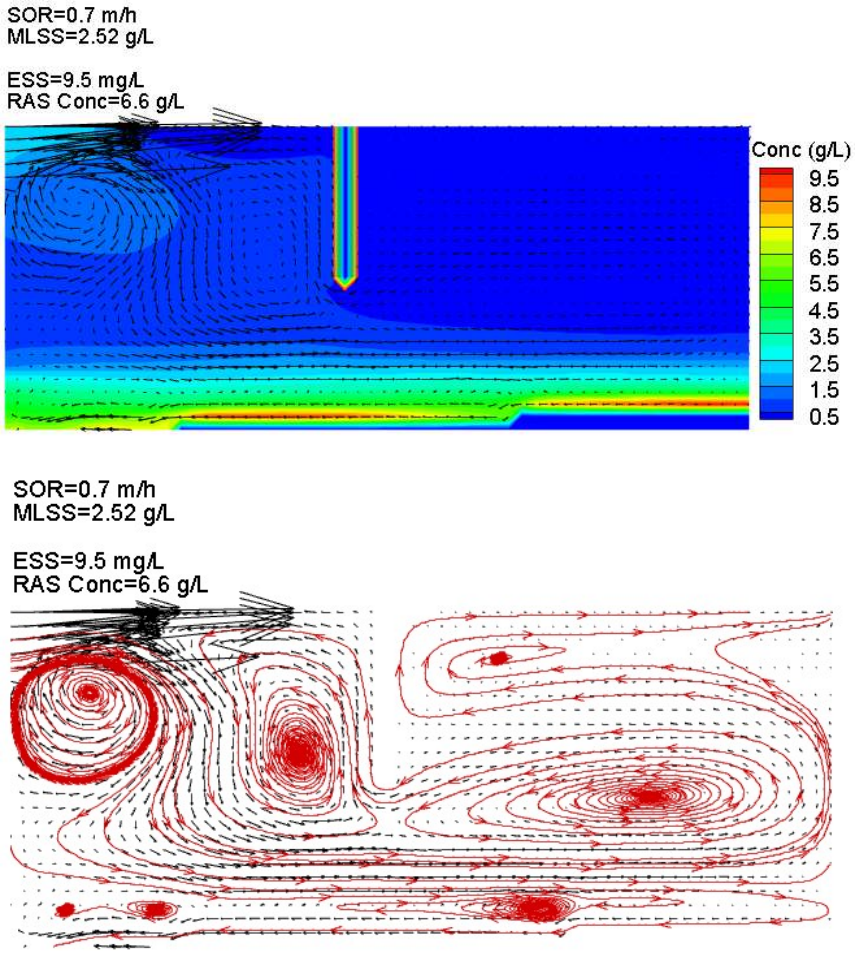

Figure 19- (a) Simulated velocities and solids distribution and (b) streamline before geometry modification (simulation 6).

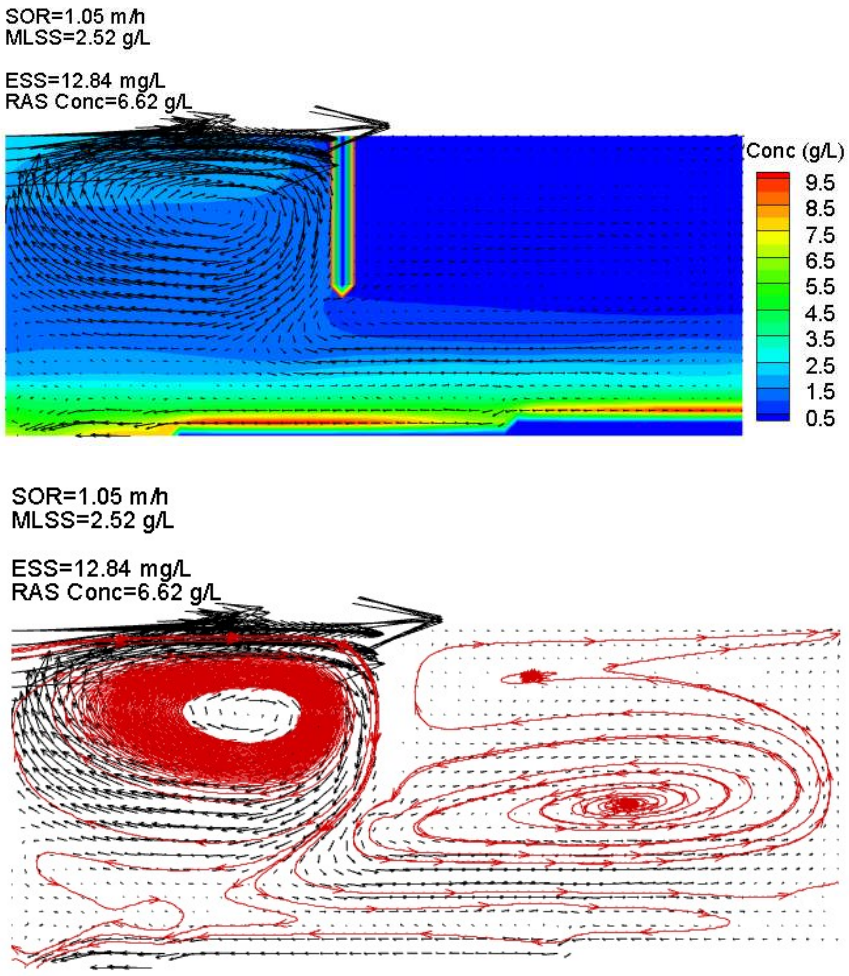

Figure 20- (a) Simulated velocities and solids distribution and (b) streamline before geometry modification (simulation 7).

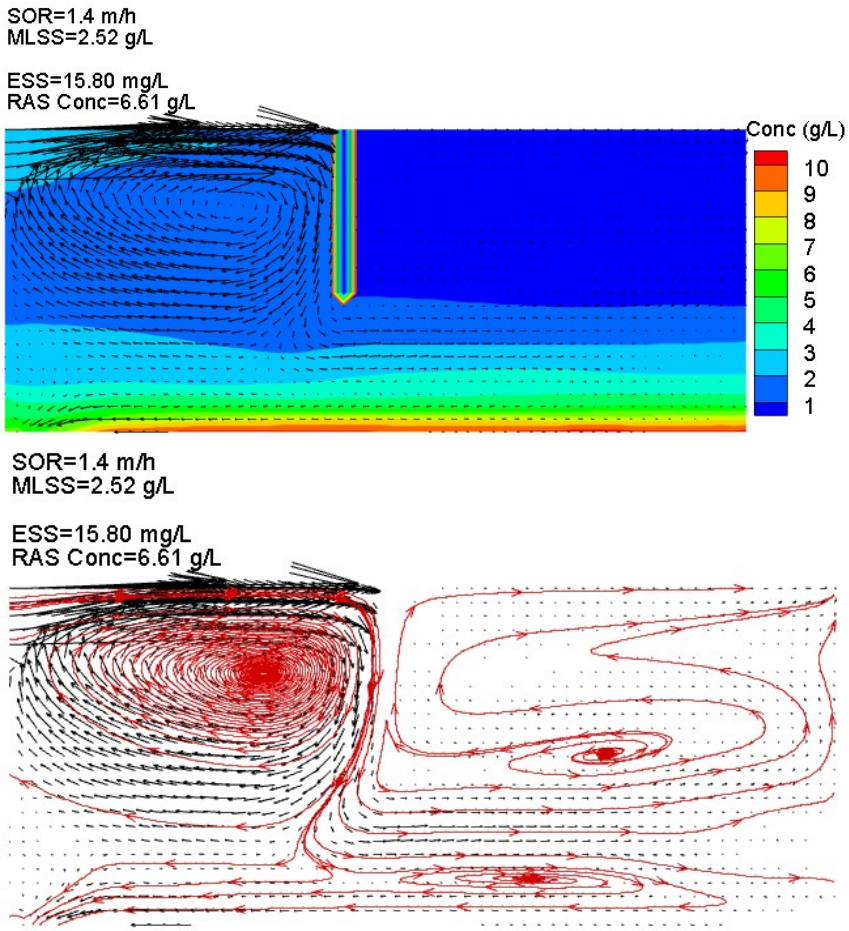

Figure 21- (a) Simulated velocities and solids distribution and (b) streamline before geometry modification (simulation 8).

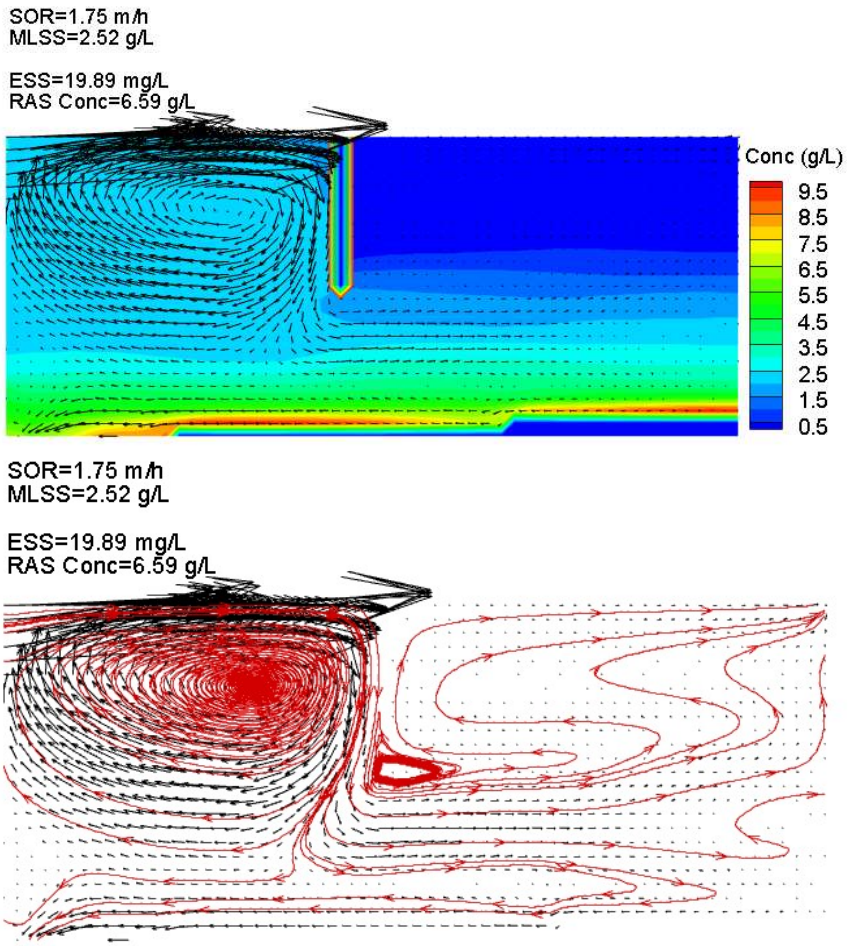

Figure 22- (a) Simulated velocities and solids distribution and (b) streamline before geometry modification (simulation 9).

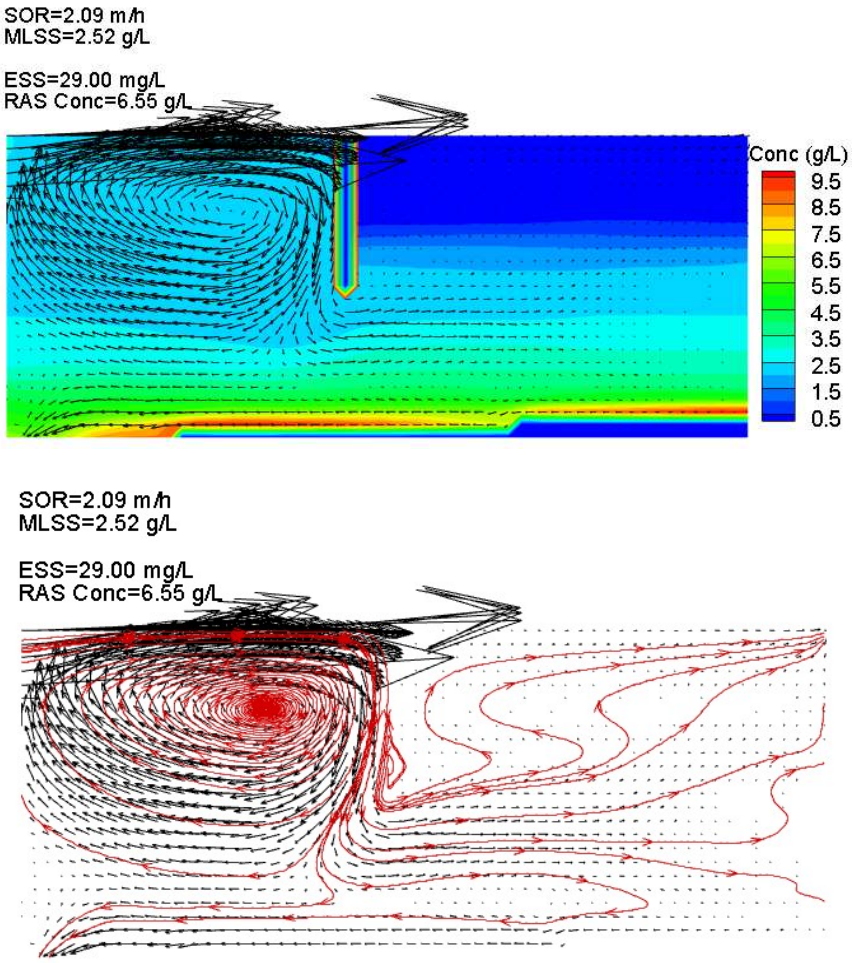

Figure 23- (a) Simulated velocities and solids distribution and (b) streamline before geometry modification (simulation 10).

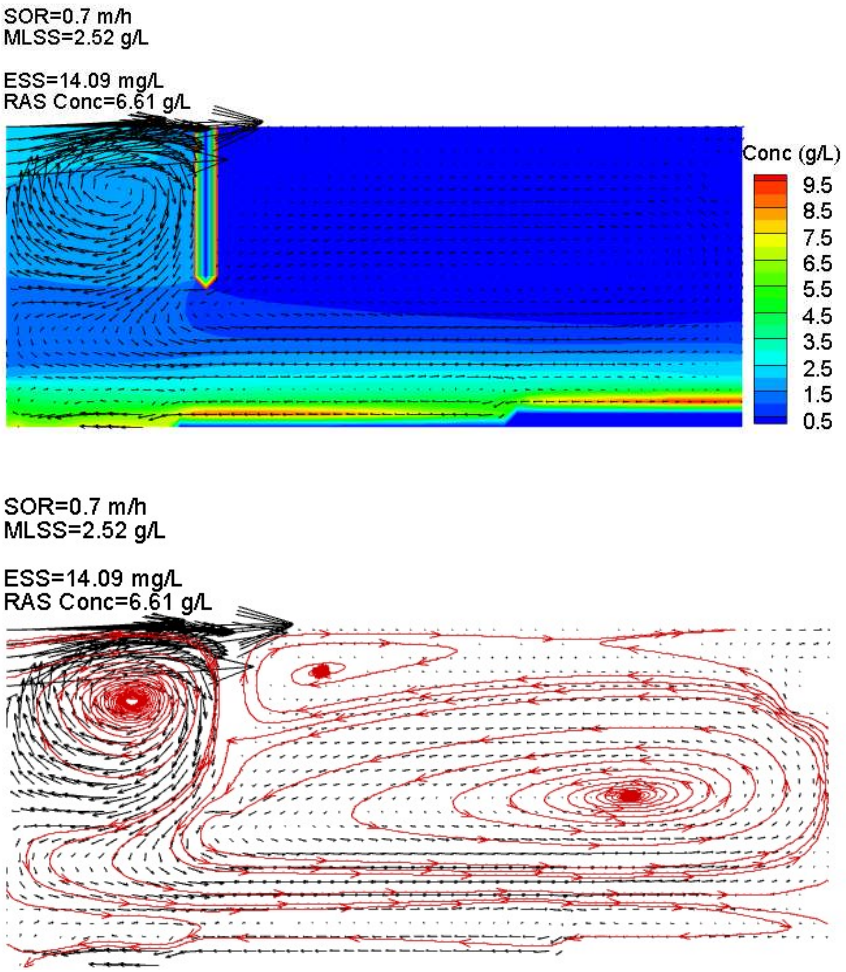

Figure 24- (a) Simulated velocities and solids distribution and (b) streamline after geometry modification (simulation 21).

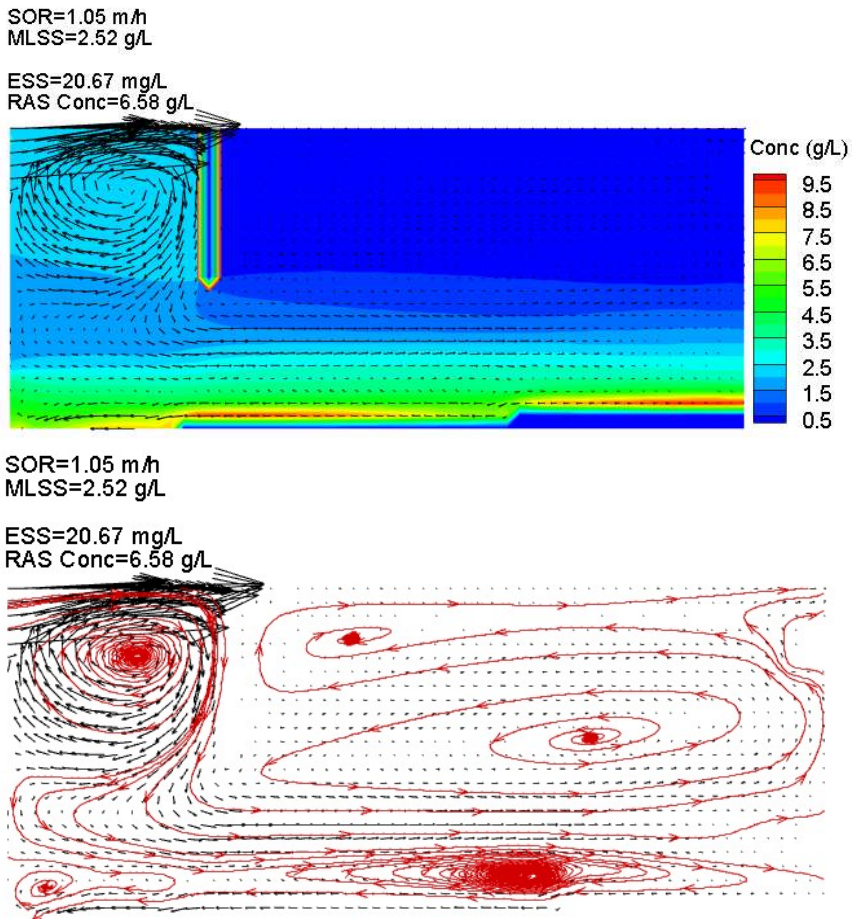

Figure 25- (a) Simulated velocities and solids distribution and (b) streamline after geometry modification (simulation 22).

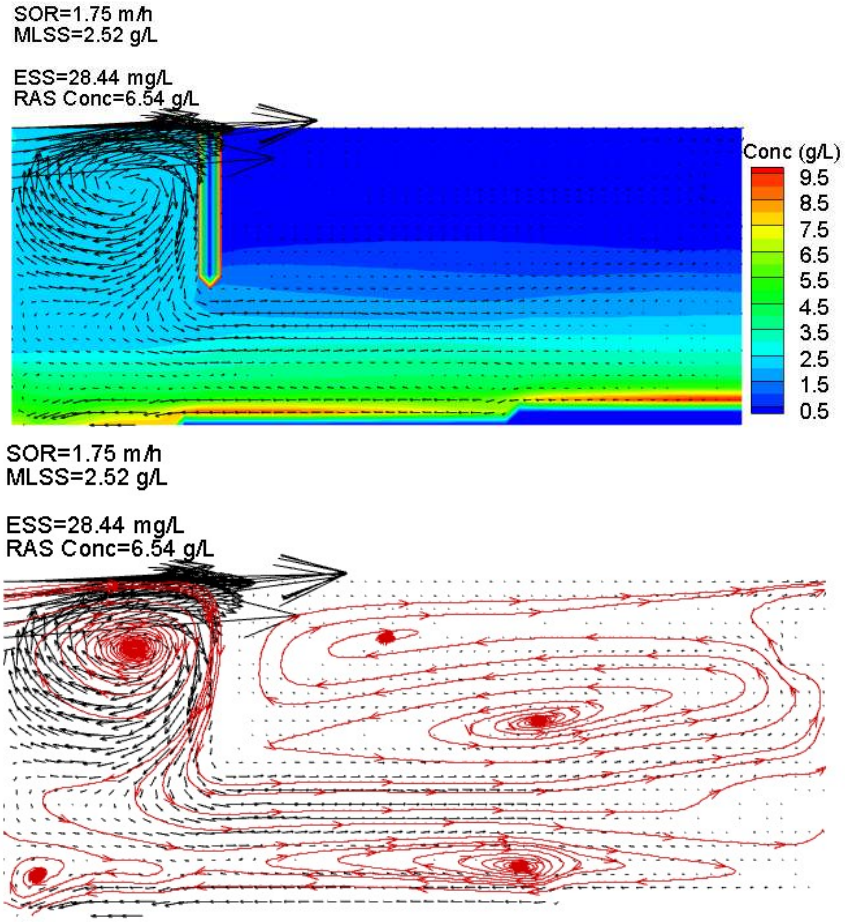

Figure 26- (a) Simulated velocities and solids distribution and (b) streamline after geometry modification (simulation 23).

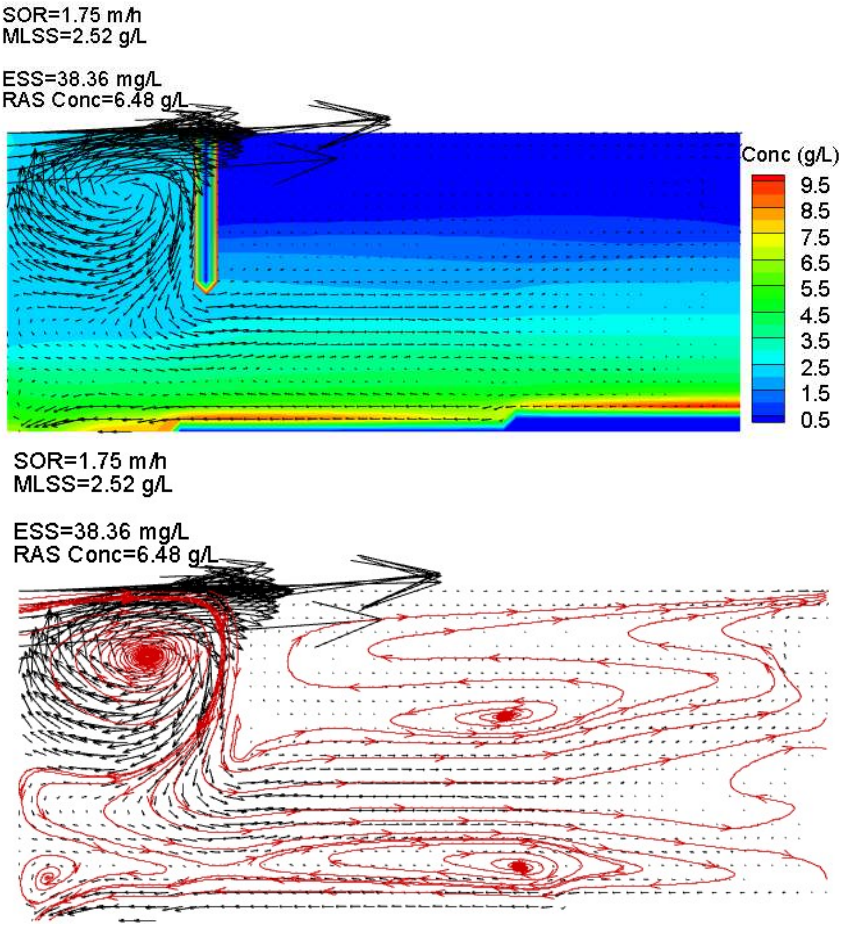

Figure 27- (a) Simulated velocities and solids distribution and (b) streamline after geometry modification (simulation 24).

Reference List

Parker, D.; Butler, R.; Finger, R.; Fisher, R.; Fox, W.; Kido, W.; Merrill, S.; Newman, G.; Pope, R.; Slapper, J.; Wahlberg, E. Design and operations experience with flocculator-clarifiers in large plants. *Water Science and Technology.* **1996**, *33, 12,* 163–170.

Kleine, D and Reddy, B. D. Finite element analysis of flows in secondary settling tanks. *Int. J. Numer. Meth. Engng*. **2005**, *64, 7*, 849-876.

Parker, D. S.; Kinnear, D. J.; Wahlberg, E. J. Review of folklore in design and operation of secondary clarifiers. *Journal of Environmental Engineering*. **2001**, *127, 6*, 476-484.

Ben, L and Stenstrom, M. K. Research Advances and Challenges in One-Dimensional Modeling of Secondary Settling Tanks - A Critical Review. *Wat. Research*. **2014**, *65*, 40-63.

Wang, X. L.; Zhou, S. S.; Li, T.; Zhang, Z. Q.; Sun, Y. X.; Cao, Y. B. Three-dimensional simulation of the water flow field and the suspended-solids concentration in a circular sedimentation tank. *Canadian Journal of Civil Engineering*. **2011**, *38, 7*, 825-836.

McCorquodale A, Griborio A, Georgiou I. A public domain settling tank model. *Proceeding of the Water Environmental Federation*. **2005**, Session 31-40, 2546-2561.

McCorquodale, J.A.; La, M. E. J.; Griborio, A.; Homes, D.; Georgiou, I. Development of software for modeling activated sludge clarifier systems. A Technology Transfer Report, Department of Civil and Environmental Engineering, University of New Orleans, LA, 2004, 70148.

DeClercq, B. (2003). Computational Fluid Dynamics of Settling Tanks: Development of Experiments and Rheological, Settling and Scraper Submodels. Ph.D. Thesis. University of Ghent, Belgium.

Fan, L.; Xu, N.; Ke, X. Y.; Shi, H. C. Numerical simulation of secondary sedimentation tank for urban wastewater. *Journal of the Chinese Institute of Chemical Engineers*. **2007**, *38, 5*, 425-433.

Liu, X. D.; Xue, H. Q.; Hua, Z. L.; Yao, Q.; Hu, J. Inverse calculation model for optimal design of rectangular sedimentation tanks. *Journal of Environmental Engineering*. **2013**, *139, 3*, 455-459.

Ramalingam, K.; Fillos, J.; Xanthos, S.; Gong, M.; Deur, A.; Beckmann, K. Development and validation of a 3-dimensional computational fluid dynamics (CFD) model form rectangular settling tanks in New York City Water Pollution Control Plants. *Water Practice and Technology*. **2009**, *4, 1*, 1-9.

Vitasovic, Z, C.; Zhou, S. P.; McCorquodale, J. A.; Kong, L. G. Secondary clarifier analysis

using data from the clarifier research technical committee protocol. *Water Environment Research*. **1997**, *69, 5*, 999-1007.

Wahlberg, E. J.; Gerges, H. Z.; Gharagozian, A.; Stenstrom, M. K.; Vitasovic, Z, C. Of: Secondary clarifier analysis using data from the clarifier research technical committee Protocol. *Water Environment Research*. **1998**, *70, 2*, 249- 253.

Taebi-Harandy, A.; Schroeder, E. D. Formation of density currents in secondary clarifier. *Wat Res*. **2000**, *34, 4*, 1225-1232.

Moursi, A. M.; McCorquodale, J. A.; El-Sebakhy, I. S. Experimental studies of heavy radial density currents. *Journal of Environmental Engineering*. **1995**, *121, 12*, 920-929.

Zhou, S.; McCorquodale, J. A. Modeling of rectangular settling tanks. *Journal of Hydraulic Engineering*. **1992**, *118, 10*, 1391-1405.

Zhou, S.; McCorquodale, J. A.; Vitasovic, Z. Influences of density on circular clarifiers with baffles. *Journal of Environmental Engineering*. **1992**, *118, 6*, 829-847.

Krebs, P. The hydraulics of final settling tanks. *Water Science and Technology*. **1991**, *23, 4-6*, 1037-1046.

Samstag, R.W.; Dittmar, D. F.; Vitasovic, Z. Underflow geometry in secondary sedimentation. *Water Environment Research*. **1992**, *64, 3*, 204-212.

Jensen, D. E.; Spalding, D. B.; Tatchell, D. G. Computation of structures of flames with recirculating flow and radial pressure gradients. *Combustion and Flame*. **1979**, *34*, 309-326.

Daigger, G. T. Development of refined clarifier operating diagrams using an updated settling characteristics database. *Water Environment Research*. **1995**, *67, 1*, 95-100.

Parker, D. S.; Kaufman, W. J.; Jenkins, D. Physical conditioning of activated sludge floc. *Water Pollution Control Federation*. **1971**, *43, 9*, 1817-1833.

Chu, I.; Griborio, A.; Pitt, P.; Ahmad, M. L.; Chiu, G.; Desai, J.; Ling, E. Combination of field testing and CFD modeling for optimum clarifier design. *Water Environmental Federation*. **2015**, 991-1025.